

# **EVAPOTRANSPIRATION FROM NATURAL AND PLANTED FOREST IN THE MIDDLE MOUNTAIN OF NEPAL**

TIKARAM BARAL  
FEBRUARY, 2011

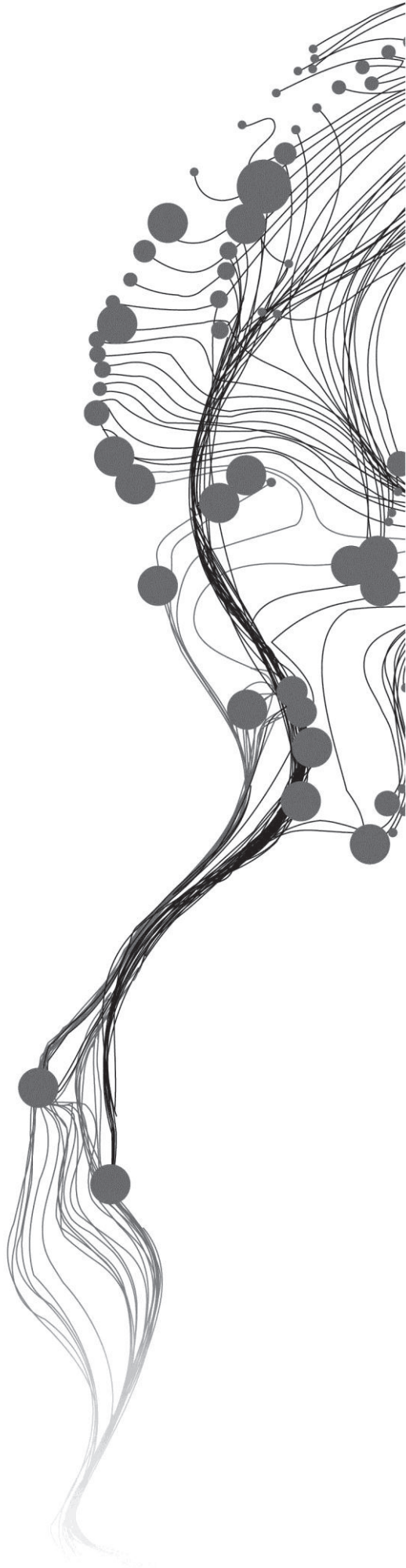
**SUPERVISORS:**

Dr. Ir. Maciek Lubczynski (First Supervisor)

Dr. Ir. Christiaan van der Tol (Second Supervisor)

**ADVISOR:**

Ir. Chandra Prasad Ghimire



# EVAPOTRANSPIRATION FROM NATURAL AND PLANTED FOREST IN THE MIDDLE MOUNTAINS OF NEPAL

TIKARAM BARAL

Enschede, the Netherlands, [February, 2012]

Thesis submitted to the Faculty of Geo-Information Science and Earth Observation of the University of Twente in partial fulfilment of the requirements for the degree of Master of Science in Geo-information Science and Earth Observation.

Specialization: Water Resource and Environmental Management

## **SUPERVISORS:**

Dr. Ir. Maciek Lubczynski (First Supervisor)

Dr. Ir. Christiaan van der Tol (Second Supervisor)

## **ADVISOR:**

Ir. Chandra Prasad Ghimire

## **THESIS ASSESSMENT BOARD:**

Prof. Dr. Z. (Bob) Su – Chairman

Prof. O. Batelaan – External Examiner (Vrije Universiteit Brussel)

Dr. Ir. Maciek Lubczynski – First Supervisor

Dr. Ir. Christiaan van der Tol – Second Supervisor

## DISCLAIMER

This document describes work undertaken as part of a programme of study at the Faculty of Geo-Information Science and Earth Observation of the University of Twente. All views and opinions expressed therein remain the sole responsibility of the author, and do not necessarily represent those of the Faculty.

## ABSTRACT

Adequate water resources for future generations are of great concern in the Middle mountains of Nepal. The demand for water is rising due to increasing population and agricultural intensifications. On the other hand, forest and land degradation are a major problem in the Middle Mountains of Nepal. Because of these degradations, several hydro-ecological problems such as floods and erosions were becoming more evident. However, also degradation of water resources was observed affecting excess flows during the rainy season and low flows during the dry season. For years, reforestation was thought to be a viable solution to restore the diminished but extremely important for local communities; dry season low flows. Therefore an intensified reforestation program was carried out in the Middle Mountains of Nepal. Though forest plays positive role with respect to erosion control, it is also responsible for the use and loss of water from the catchment. This research focuses on the estimation of individual water uses by planted forest, natural forest and degraded land in the Middle Mountains of Nepal and their comparison.

For the purpose of the comparative study, planted forest, natural forest and degraded pasture land were chosen in the Jikhu Khola Watershed in the Middle Mountains of Nepal. The methodology included measurements and estimation of: i) interception loss from natural and planted forest stands; ii) transpiration from natural and planted forest; and iii) evaporation from the degraded pasture land. The period under investigation lasted from October, 2010 to September, 2011, covering a whole hydrological year. Finally, remote sensing based SEBS model was run for two days of Landsat overpass and compared with the pixel of the interest representing the three stands in the study area.

Gash model was used to calculate the total annual interception loss from natural and planted forest stands whereas sap flow measurements were used to estimate the total annual transpiration from the both forest stands. Sap flow was calculated as the product of sap flux densities measured with Thermal Dissipation Probe (TDP) and sapwood area. The radial sap flow patterns were derived using the Heat Field Deformation (HFD) sensor. The TDP measurements were radially corrected using the radial sap flow patterns derived from HFD measurement. Cienciala mode was used to extrapolate the sap flow data for the period when there were no measurements. Biometric Upscaling Function (BUF) was used to obtain the stand level tree transpiration.

The total annual ET was 566 mm, 495 mm and 206 mm for pine forest, natural forest and degraded pasture respectively. The results showed that despite high interception loss in the natural forest due to its high density, the total annual ET was high in the pine forest. The high ET in pine forest is attributable to its large dry season transpiration rate ( $1 \text{ mmday}^{-1}$ ), significantly larger than in wet season ( $0.42 \text{ mmday}^{-1}$ ). ET is the lowest in case of degraded pasture land ( $0.56 \text{ mmday}^{-1}$ ). The output from the SEBS showed reasonably good agreement with the bare soil evaporation but poor results with the forest stands probably associated with the non-representative meteorological parameters.

The larger evapotranspiration from the planted pine forest than from the natural forest or degraded land is likely the reason of drying water resources in the middle mountains of Nepal although more research need to be dedicated to support that statement.

## ACKNOWLEDGEMENTS

The first and foremost gratitude goes to my first supervisor Dr. Maciek Lubczynski for his support throughout the work. His guidance, suggestion and critical comments were very fruitful to bring my work into this form. I would like to thank my second supervisor Dr. Christiaan van der Tol for guiding and reviewing my work and helping during my fieldwork preparation.

I am very thankful to my advisor Chandra Ghimire for helping, guiding and supporting me with comments and suggestions throughout my work from the first day of my proposal until the completion of my work.

I would like to appreciate and thank to Dr. Boudewijn de Smeth for helping me to carry out laboratory analysis. I am grateful to Joris Timmerman for helping with the Matlab code which was very helpful for handling the bulk datasets. Also I want to thank to Mostafa Gokmen for helping me in the last hour. Thanks also go to Zoltan vekerdy, Ben Mathuis for helping in Ilwis and Chris Mannerts for providing the data of the study area.

I am very thankful to all the members of department of water resources including the professors and staffs for providing a joyful environment to carry out this M Sc degree.

My sincere thanks also go to all the members of Nepali Society for their love and it was really a great environment to be together. Thanks to Phuong and Yeti for encouragement and spending wonderful time together and all my friends in Water Resource department and ITC.

Finally, my acknowledgement goes to the Netherlands Fellowship Program (NFP) for funding my studies and Department of Irrigation, Nepal for providing me the study leave.

# TABLE OF CONTENTS

---

List of Figures.....	iv
List of Tables.....	v
1. Introduction.....	1
1.1. Background.....	1
1.2. Problem definition .....	1
1.3. Objectives and research questions .....	2
1.4. Significance of the study .....	3
1.5. Assumptions.....	3
2. Literature review .....	4
2.1. Reforestation, evapotranspiration and drying water resource .....	4
2.2. Existing method of estimating evapotranspiration .....	4
2.3. Transpiration using sap flow .....	6
2.4. Rainfall interception.....	10
2.5. Evaporation from degraded land.....	12
2.6. Surface Energy Balance System: .....	13
3. The study area .....	14
3.1. Location .....	14
3.2. Land use and land cover.....	15
3.3. Climate and hydrology.....	16
4. Methodology.....	17
4.1. Data collection .....	18
4.2. Sap flux density and biometric parameters .....	18
4.3. Gash analytical model.....	21
4.4. Evaporation from degraded pasture land .....	22
4.5. Evapotranspiration from SEBS .....	23
4.6. Standard meteorological data .....	25
5. Results.....	27
5.1. Rainfall interception.....	27
5.2. Stand level transpiration .....	29
5.3. Evaporation from degraded soil .....	40
5.4. Annual evapotranspiration from natural forest, pine forest and degraded pasture.....	41
5.5. Evapotranspiration from SEBS .....	42
6. Discussions and conclusions.....	43
7. Recommendations .....	46

## LIST OF FIGURES

Figure 1: Thermal Dissipation Probe for measuring sap flux velocity .....	8
Figure 2: Heat Field Deformation for measuring Sap flux density .....	8
Figure 3: Physiographic regions of Nepal .....	14
Figure 4: Location map of the study area.....	15
Figure 5: Location of Degraded Pasture (Top left), Pine forest stand (Top right) and Natural forest stand (bottom).....	16
Figure 6: Flowchart of the methodology.....	17
Figure 7: Thermal insulation provided in the sensors for preventing from NTG .....	19
Figure 8: A cross section of a pine tree (left) and <i>Castanopsis tribuloides</i> (right) showing sapwood, heartwood and bark (Source: Ghimire, C, Personal Communication .....	19
Figure 9: Tree boring for sapwood area determination (left) and obtain sample (right) .....	20
Figure 10: Rainfall distribution in NFS and PFS.....	21
Figure 11: Estimation of canopy parameters S and p using the method of Jackson (1975) for pine forest (Ghimire <i>et al.</i> , 2012).....	22
Figure 12: Methodology applied for SEBS .....	24
Figure 13: Daily average solar radiation, relative humidity, and wind speed and maximum and minimum temperature measured in the study area from September, 2010 to August, 2011 .....	26
Figure 14: Contribution of components of Gash model to total interception loss.....	28
Figure 15: Sap flux density in three pine trees showing strong correlation with the incoming solar radiation .....	30
Figure 16: NTG Monitoring using unpowered TDP in three different locations of pine forest (Top and bottom left) and one location in natural forest (bottom right).....	31
Figure 17: Circumferential (Top and bottom left) and axial (bottom right) variation of sap flux density in Pine trees monitored using TDP .....	31
Figure 18: Sap flux density in Cienciala model calibration (left) and validation (right), starting from top to down pine tree in dry season, pine tree in wet season, natural tree in dry season and natural tree in wet season .....	34
Figure 19: BUF for Pinus (left) and <i>Castanopsis tribuloides</i> (right) with a least square linear fit.....	35
Figure 20: Relationship between sapwood area and sap flux density in the dry (left) and wet (right) seasons in the PFS .....	35
Figure 21: Relationship between sapwood area and sap flux density in the dry (left) and wet (right) seasons in <i>Castanopsis tribuloides</i> of the NFS .....	36
Figure 22: Radial profile of sap flux density in pine tree (left) and natural tree (right) obtained from HFD measurements .....	36
Figure 23: Derived BUF in four stands of pine .....	39
Figure 24: Observed and modelled soil moisture content during calibration (left) and validation (right) in Hydrus.....	40
Figure 25: Soil moisture profile at 10 cm, 25 cm, 50 cm and 75 cm in June, 2011 (upper graph) and January, 2011 (lower graph).....	41

## LIST OF TABLES

Table 1: Terminology used in Gash Interception Model.....	11
Table 2: The original and revised analytical Gash Model equations (Gash. <i>et al.</i> , 1995).....	12
Table 3: Site information of the three stands.....	15
Table 4: Data collected and measured.....	18
Table 5: Landsat ETM+ bands .....	23
Table 6: Parameters of the revised Gash Model derived by Ghimire <i>et al.</i> (2012) in the study area.....	27
Table 7: Total Interception loss in two stands, in mm.....	27
Table 8: Sensitivity analysis model parameters in Gash model.....	28
Table 9: Biometric properties of trees monitored in PFS and NFS (values associated with dry and wet indicates the total number of trees used for the analysis in the wet and dry seasons) .....	29
Table 10: Average sap flux density in circumferential direction of pine trees .....	32
Table 11: Pearson Correlation coefficient between Js and RH and Rs.....	32
Table 12: Model parameters and associated errors in two seasons of both stands .....	33
Table 13: Proportion of sap flux density integrated over the entire sap wood depth and depth of TDP measurement .....	37
Table 14 Factors for radial correction of sap flow in different categories of pine and natural trees.....	37
Table 15: Dry and wet season transpiration in PFS and NFS.....	38
Table 16: Spatial variability of sap flow in the study area .....	39
Table 17: Textural properties and bulk density of soil in the degraded pasture land.....	40
Table 18: Initial parameters for Hydrus model simulation and associated objective function .....	40
Table 19: Total dry and wet season top and bottom flux in the degraded soil .....	41
Table 20: Annual ET in PFS and NFS.....	41



# 1. INTRODUCTION

## 1.1. Background

The increase in the human trampling and livestock pressure over the natural forest beyond its capacity has accelerated the degradation of forest ecosystem in the tropical part of the world. The high dependence of the rural population on fuel wood and indiscriminate falling of trees and expansion of agricultural land by clearing forest are the major causes of land degradation in the developing countries like Nepal (Karkee, 2004). These degraded lands are hydrologically unstable due to excess flow during the rainy season and water shortages during the dry season. Parrotta (1992) characterized the degraded land as impoverished or eroded soils with reduced primary production and diminished biological diversity.

The degradation has been influencing the water yield from the forest due to which it is creating global stress on water supply (Trabucco *et al.*, 2008) and increased nutrient and sediment load in the rivers (Herron *et al.*, 2002). This demands an effective water management strategy for social and economic development (Fregoso, 2002) and reforestation for sustainable development of water resource. At the same time it is also necessary to understand possible hydrological impact of the reforestation. This requires a better understanding of the complex hydrological cycle and the factors governing them.

The change in the vegetation cover influences water yield of the catchment, through changes in infiltration, interception, evaporation and transpiration. The change in land use affects all these components. However, evapotranspiration (ET) is considered to be the most important hydrological components affected by reforestation which influence the annual runoff of the catchment (Komatsu *et al.*, 2011). The reforestation impacts on hydrology differs with species (Bosch and Hewlett, 1982), climatic conditions (Sun *et al.*, 2005) and topography (Riekerk, 1989). The hydrological effect of reforestation depends on whether the gain through increased infiltration overweighs increased ET (Bruijnzeel, 2004) and how it effects the stream discharge. The decrease in net annual yield is attributable to the increased evapotranspiration (Riekerk, 1989) after reforesting the degraded pasture.

There are many methods developed to estimate the evapotranspiration or components of ET across a spectrum of spatial scales ranging from individual plants, soil samples and soil profiles to the atmospheric surface layer and the entire watershed (Wilson *et al.*, 2001). These methods are mostly based on the physics involved in the process or water balance and energy balance approach. As evapotranspiration is considered to be the most difficult component to estimate, the ET assessments methods have certain strengths and limitations depending upon the methods applied and assumptions used (Cammalleri *et al.*, 2010; Rana and Katerji, 2000). Therefore, the selection of the appropriate method is challenging particularly at the catchment scale characterized by different land use and topographic conditions.

## 1.2. Problem definition

Bruijnzeel (2004) highlighted that the water use capacity of newly planted trees is more than the natural forest and therefore the change in yield can be more distinct. Similarly, the claim on conversion of coniferous forest to broad leaf forest to increase the annual runoff due to the diminished evapotranspiration is questionable (Komatsu *et al.*, 2011) and it is valid in case of areas with high winter

rainfall (temperate region) but not in case of the area having lower winter rainfall (Komatsu. *et al.*, 2009). Most of the analysis in the tropical forests like in Nepal is based on the literatures from the study of temperate regions or tropical regions where the rainfall pattern is different. The rainfall pattern in the present study is highly seasonal with about 80% of annual rainfall occurring during rainy season from June-September (Merz, 2004). Hence, the quantification of the water budgets of the forest in the Middle Mountains, where the climate is significantly different from that in the temperate region, is a critical research topic. This helps to understand how the reforested plantation changes the annual yield. This not only helps to quantify total water uptake by trees but also helps to compare water uptake of natural and reforested plantation.

There are some issues which are needed to be addressed while assessing the hydrological impact of reforestation. What is the amount of water transpired by the vegetation? Does the rate of transpiration of the planted forest same as the natural forest? What is the spatial variability of the transpiration? The spatial variability becomes more important in the hilly and mountainous areas where representing the spatial variability of the factors influencing evapotranspiration is difficult. Similarly, the contribution of evaporation to the ET increases with the introduction of new plants in the degraded soil. So, the variability in the contribution of evaporation and transpiration with reforestation is also important to be carried out. The evaporation from the degraded land is also equally important to assess how the reforestation has changed the ET from its original degraded condition. Some of these issues had been addressed in some literatures, but generalization is made with the forest cover, considering all the species, natural and planted canopy the same or some of them limited with the transpiration or evaporation measurement only. Therefore, it is necessary to independently quantify the major factors associated with the ET, define its temporal variability and also the variability with respect to the land cover.

Reforestation program had been carried out in the Middle Mountain of Nepal since last 30-40 years after some extreme effect of land degradation in the form of erosion and high flood was experienced. However, very limited work has been done to address the impact of this reforestation on the hydrology besides its positive impacts like protecting downstream from natural hazards. Modelling overall evapotranspiration at the catchment scale doesn't indicate the species specific effect on the overall hydrology. Therefore, the necessity of independently quantifying the evapotranspiration of the natural forest and the reforested pine forest has motivated to conduct this study.

### **1.3. Objectives and research questions**

#### **Main Objective:**

To evaluate the hydrological impact of pine plantation in the formerly degraded pasture by estimating the changes in vegetation water use in the Middle Mountains of Nepal

#### **Specific Objectives:**

To estimate the soil water uptake by pine plantation and natural forest and upscale it to the Hill slope stand.

To estimate the interception loss by the pine plantation and natural forests

To estimate the evaporation in the degraded pasture land

To develop dry and wet season evapotranspiration on pine forest, natural forest and degraded land and compare the seasonal variability.

To compare the values of ET estimated using SEBS and field measurement

### **Research Questions:**

What is the extra water uptake by the planted pine forest as compared to the natural forest?

What is the spatial variation of tree transpiration rate within the catchment?

What is the total dry and wet season evaporation rate at hill-slope level?

What is the seasonal variation of evapotranspiration in natural and planted forest and degraded land?

## **1.4. Significance of the study**

This study is intended to quantify the evapotranspiration from the forest and the degraded pasture land in the Middle Mountains of Nepal. The specific objective of the study is to directly measure the transpiration and evaporation from the planted and natural forest, identify the factors influencing it and to calculate the evaporation from degraded pasture lands using meteorological and soil physical parameters. This work can be a good initiative towards understanding the effect of reforesting the degraded land in the hilly slopes in Nepal. This also helps to understand the transpiration and interception loss contributed by the different species in the middle mountain. This work also helps to develop the datasets of the evapotranspiration in the middle mountain area of Nepal, which is to the best of our knowledge, are not available yet.

## **1.5. Assumptions**

Most of the annual evapotranspiration (ET) estimation has been done with a single method with assumption and simplification of the method or model applicable throughout the dry and wet season. Evapotranspiration is the sum of the transpiration and the evaporation. Therefore, independent measurement of transpiration and evaporation can be a more promising method to obtain ET by combining the two methods. This help to make the comprehensive science based evaluation of the hydrological effect of reforestation. Therefore, the study was carried out with the following assumptions:

- The total evapotranspiration (ET) in forest is equal to the sum of the transpiration from the tree and the evaporation from the intercepted water. The other components contributing to the total ET such as evaporation from the soil profile, understory plants are negligible.
- ET from degraded pasture is equal to the evaporation from unsaturated soil zone.
- Meteorological measurement at a single location of the study area is representative for all the stands.

## 2. LITERATURE REVIEW

### 2.1. Reforestation, evapotranspiration and drying water resource

The influence of deforestation and reforestation on water supplies has long been a concern of the scientific community and society. The ecological benefit of the forest has been well established however the hydrological impact of the reforestation is unclear (Xiaohua *et al.*, 2007). These effects can be different due to different catchment hydrological process controlled by climate, soil, topography and tree species and age.

The hydrological effect of reforestation in a catchment can be understood by the water balance equation where the total incoming rainfall is equal to the sum of evapotranspiration, runoff and change in storage. The increase of tree abundance increases evapotranspiration where removal decreases. Therefore, deforestation results in decrease in ET; which means more water is available for groundwater recharge and runoff (Riekerk, 1989) and thus results in more water yield. At the same time, the clearance of the forest alters the soil hydraulic properties like infiltration capacity, which may reduce the recharge to the ground water and thus drying of water resource may occur. Therefore, it is necessary to understand the effects on every component of the water balance in order to understand how reforestation affects the water yield.

Adnan and Atkinson (2011) found the main reason of increased frequency and magnitude flooding in Malaysia is due to the change of precipitation as well as land use. The changes in land use such as deforestation imply reduction of evapotranspiration and increase of the rainfall contribution to runoff. The reduction in the forest area in the mountainous regions like Nepal can bring similar extreme floods during the rainy seasons. The mountainous area having high rainfall and low temperature has higher yield compared to the coastal area dominated by wetlands receiving lower rainfall but high evapotranspiration (Sun *et al.*, 2005). Therefore, evapotranspiration becomes one of the important factors to be estimated whenever there is land cover change. However, the influence of the land cover on other components of the water balance can't be ignored.

### 2.2. Existing method of estimating evapotranspiration

There are many methods to directly or indirectly measure or estimate ET or components of ET. The ET measurement methods are based on hydrological approaches (e.g. soil water balance, weighing lysimeters), micrometeorological approaches (e.g. Energy balance and Bowen ratio, aerodynamic method, eddy covariance) or plant physiology approaches (e.g. sap flow method, chamber method). Similarly, the evapotranspiration estimation methods are based on analytical approach (e.g. Penman-Montheith model) or empirical approach (e.g. Crop coefficient method). A review of these methods has been documented by Rana and Katerji (2000). All these methods have some limitations and strength. The best suited method should be selected based on the availability of the data, accuracy or cost incurred or time and space scales.

Soil water balance method applies the principle of conservation of mass where the water balance components are measured or estimated. Evapotranspiration is obtained as the residual from a simple water balance equation in which precipitation equals to ET plus surface runoff and change in the soil moisture storage. In order to obtain the high accuracy in the estimation of ET, it is essential to measure the components accurately which is a difficult task. Similarly, irrigation water, contribution from the ground water and drainage are also needed to be incorporated in the equation for higher precision, which adds more complication in applying the water balance equation. This method is applicable in the spatial

extend of 10 m<sup>2</sup> to 10 km<sup>2</sup> and temporal period of a week to a year (Rana and Katerji, 2000) and accuracy of the method is dependent on the spatial and temporal measurement of soil moisture (Burrough, 1989).

Lysimeters are devices to measure ET directly by mass balance of water (weighing lysimeters) or indirectly by volume balance (non-weighing lysimeters) with the sensor inside the tank in a field measuring the change in the weight variation due to ET. This is a point measurement (Gebet and Cuenca, 1991) and may not be representative for the spatial extent in the area with non-homogeneous land use. The accuracy of lysimeters varies from 10% at a daily scale to 10-20% at the hourly scale (Klocke *et al.*, 1985) in the temperate climate. It is also not suitable for deep soil and for arid and semi-arid regions where heating of metallic rim may influence ET significantly (Rana and Katerji, 2000).

The energy balance equation where the net radiation is equal to the sensible heat flux, latent heat flux and ground heat flux is used to estimate the ET by energy balance and Bowen ratio method. This method has been applied in large field condition and within 10% in accuracy (Rana and Katerji, 2000) and more suitable in semi-arid environment (Dugas *et al.*, 1991). This method is easy to apply and requires the measurement of temperature and humidity at two levels, net radiation and soil net flux (Lui and Foken, 2001).

The aerodynamic method is applied from the measurement of the specific air humidity and wind speed over the atmospheric profile. The main limitation of the method is correctly measuring the vapour pressure at the different height (Rana and Katerji, 2000).

The chamber method is the field measurement method ET. In this method an aluminium conduit covered with Mylar film is mounted in a tractor. Air is circulated continuously from the fans mounted near the chamber bottom. ET rate is calculated from the air and wet bulb temperatures of a thermistor psychrometer from the initial vapour pressure before placing the chamber and after the chamber is operated. The method is explained in detailed by Reicosky and Peters (1977) and is claimed to obtain up to 10% accuracy. This method is not suitable for long term ET estimation and the high cost limits its' use for a short period (Rana and Katerji, 2000). This method is not portable and usually alters the micro climate (Smith and Allen, 1996).

The Penman-Montheith method recommended by FAO Allen *et al.* (1998) has received wide acceptance for estimating evapotranspiration (Liu and Liu, 2007). It uses equations of energy fluxes and transfer of heat and water vapour between land surface and the atmosphere (Steward, 1989). The empirical method estimates the evapotranspiration as a fraction of the reference evapotranspiration developed independently. The most common method is to develop crop coefficient (Kc) value based on the land cover and estimate the reference ET by Penman-Montheith model.

The sap flow method is the direct measurement of the plant water use with the use of the sensors. There are many methods developed to measure the sap flow based on principles of thermodynamic, electric, magneto-hydrodynamic and nuclear resonance (Čermák *et al.*, 2004) but only few are widely used. Detailed review of this method is presented in the next section. This methods is applicable for the measurement of the transpiration only, therefore, the other components of the ET need to be assessed separately.

Most of the above mentioned ET estimation is point measurement methods or the methods with small spatial coverage. It may not be feasible for large-scale or regional based evaluation. Therefore, methods based on remote sensing are getting more popularity due to its high spatial coverage. SEBS proposed by Su (2002) is one of the remote sensing based ET estimation method.

### 2.3. Transpiration using sap flow

Many of the hydrological studies, the water loss from the soil plant system are integrated into evapotranspiration, which is not always justified. In case of the situation like reforested land, the contribution of evaporation and transpiration to the changed ET is not same, as transpiration plays more roles. Therefore, independent quantification of the transpiration is more significant in these cases. For this reason sap flow methods is more importance than any other for quantifying the transpiration (Smith and Allen, 1996). Transpiration using the sap flow is the plant physiology method where the total water use by a plant is obtained from the direct measurement with sensors inserted into the plants. The measurement techniques applies a thermodynamic principle in which heat is supplied into the water conducting area of the tree or stem and obtain the flow rate or flow velocity of sap from the balance of fluxes of heat into and out of the heated section. Tree transpiration is quantified as the sap flow estimated as a product of sap flux density and xylem area. The accuracy of the sap flow is determined by the accuracy of the measurement of the sap flux density ( $J_s$ ) and xylem area ( $A_x$ ) (Bieker and Rust, 2010).

#### 2.3.1. Measurement of sap flux density ( $J_s$ )

There are many methods developed for the sap flow measurement. Čermák *et al.* (2004) listed the main methods for the sap flow measurements as Heat Pulse Velocity (HPV), Trunk Segment Heat Balance (THB), Stem Heat Balance (SHB), Heat Dissipation Probe (TDP) and Heat Field Deformation (HFD). Depending on the methods, the measurement is taken in a part or whole of the sapwood. Some methods are invasive or some non-invasive, some are suitable for small diameter stem or some for big trees. Also some cannot measure below a threshold of sap velocity while some can be used for very small sap flow and also reverse flow (Fernandez, 2011). Therefore, the appropriate methods should be selected understanding the advantage and limitations of the methods. These methods has been explained by Marshall (1958), Granier (1987), Baker and Van Bavel (1987), Jones *et al.* (1988), Čermák *et al.* (2004), Nadezhdina *et al.* (2002a) and Fernandez (2011). Among these methods, the methods based on the thermodynamic principles are widely used as they are commercially available (Čermák *et al.*, 2004; Lu *et al.*, 2004; Lubczynski, 2009) with TDP and the HFD the most common methods (Steppe *et al.*, 2010). These methods are automated process with high temporal resolution (Smith and Allen, 1996). A brief review of TDP and HFD is presented in the next section.

The thermodynamic methods of measuring sap flux density are sensitive to external heat perturbations (Lu *et al.*, 2004). The assumption that the combination of wood sap is in thermal equilibrium with the tree trunk and the heat applied is only the cause of temperature difference between the sensors may not be correct (Rincon *et al.*, 2009). Thus natural or ambient thermal gradient along the trunk may exist which can significantly affect the sap flux density (Do and Rocheteau, 2002b). The effect of Natural Thermal Gradient (NTG) can be seen if the measurements are taken close to the soil surface or near the sunrise and sunset (Lu *et al.*, 2004; Reyes *et al.*, 2011) or the study area is sparse vegetation where the tree trunks or stems can get the direct solar radiation or in arid or semi-arid environment where the trunk heat storage condition is caused due to night and day temperature variation (Rincon *et al.*, 2009) The resulting error can sometime exceed 100% (Do and Rocheteau, 2002b). Therefore, presence of NTG needs to be monitored and if present necessary corrections in the measured sap flux density need to be carried out.

The remedial and corrections methods have been proposed by some of the researcher after the realization of the NTG effect on sap flux density. For the remedial measures, it is advisable to provide the thermal and radiant insulation to sensors (Do and Rocheteau, 2002b). For the correction of the NTG, Köstner *et al.* (1998) suggested to measure the neighbouring tree and apply the correction for rest of the tree or the measure the same tree at different time than the time of sap flow measurement. This method doesn't

seems effective as NTG can have seasonal variation (Lu *et al.*, 2004). Čermák and Kučera (1981) proposed to provide extra thermocouple to measure NTG in a non-heated area of the trunk and make necessary correction. This was further adapted by Goulden and Field (1994) to make automatic correction of the NTG by integrating the thermo couple into the system. This method gave good results but requires NTG to be relatively constant along the trunk and stem sufficiently large, which is not possible in all the cases (Lu *et al.*, 2004). Do and Rocheteau (2002a) develop a transient heating method in which the sensor is provided with alternative cycle of heating and cooling for 15 min each. This method is comparatively successful in addressing the problem of NTG and gives the high accuracy in sap flow measurement (Isarangkool *et al.*, 2009; Lu *et al.*, 2004). However, this reduces the high temporal resolution of the sensors to two readings per hour.

The TDP sensor measures the sap flux density at 2 cm depth of the stem on one direction and a point of a tree. However, the trees uptake water through its entire sapwood, the measurement at a point can't be the representative for the entire sapwood as it can vary significantly along the circumference, axial and radial direction (Lu *et al.*, 2004). Therefore, these variation can't be disregarded as it can create significant errors (Čermák *et al.*, 2004; Gebauer *et al.*, 2008; Lubczynski, 2009) sometimes more than 100% (Ford. *et al.*, 2004; Nadezhdina *et al.*, 2002b).

Hatton *et al.* (1990) described a method in which radial profile of sap flux density can be obtained from a number of sensors inserted into different depth of the sap wood and developing the weighted proportion of each sapwood depth to the total sap flow. Similarly, the measuring points can be used to obtain an equation of a fitted curve which can be integrated into the sapwood (Nadezhdina *et al.*, 2002a) and the HFD sensor can be used to obtain the sap flux density at different depth. This fit can give linear (Bernier *et al.*, 2002) to least square polynomial fit (Hatton *et al.*, 1990).

The radial variation can also be accounted by applying the point-to-area method, in which the correlation between the total flow of the tree and sap flux density measured at the depth where it is maximum is established (Lu. *et al.*, 2000; Nadezhdina *et al.*, 2002a). The radial pattern is obtained with a long sensor with multiple measuring points along the stem and the correction factor should be calculated from the slope of best fit lines between the half-hourly or hourly values of sap flux density where it is maximum to account for high the temporal variation of sap flux density (Lu *et al.*, 2004). This method can also be used to develop the radial profile function with respect to the sap wood depth of maximum density like Gaussian function (Ford. *et al.*, 2004) or Weibull function (Gebauer *et al.*, 2008). The radial pattern of sap flux density varies with the species (Gebauer *et al.*, 2008) and time (Ford. *et al.*, 2004), therefore, need to be developed considering the species and time dependent radial profile.

The circumferential variation (CV) can be seen in isolated trees (Lu *et al.*, 2004), in drought and water supply condition (Lu. *et al.*, 2000). Similarly, the axial variation exists when the measurement is taken at high position of the trees (Lu *et al.*, 2004) or broadleaf trees with unevenly distributed branches (Lu. *et al.*, 2000). This variation should also be integrated into the measured sap flux density.

### 2.3.2. Thermal dissipation probe (TDP) and Heat field deformation (HFD)

The Thermal Dissipation Probe (TDP) proposed by Granier (1987) measures sap flux density which is converted to volumetric flow rate by multiplying it through active sapwood area. The TDP consist of two thermocouple needles one upper heated probe and other lower unheated probe. The probe needles measure the temperature difference ( $\Delta T$ ) between the heated needle and the sapwood ambient temperature (Fig 2.1). The  $\Delta T$  variable and the maximum  $\Delta T_{\max}$  at zero sap flow provide a direct conversion to sap flux density from Equation 1. The power of the heating element is 0.2 watts (Dynamax

Inc, 1997). The TDP are relatively cheap and easy to manufacture and are readily interfaced with data loggers for remote operations (James *et al.*, 2002).

$$J_s = 0.0119 \left( \frac{\Delta T_{\max} - \Delta T}{\Delta T} \right)^{1.231} \quad 1$$

Where,  $\Delta T$  is the temperature difference at the flow condition and  $\Delta T_{\max}$  is the temperature difference between the two probes at no flow condition.

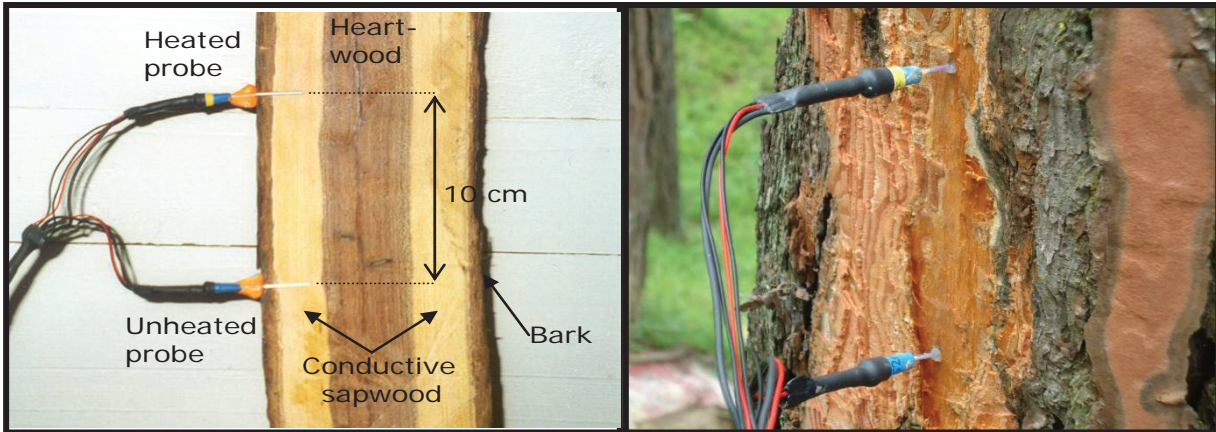


Figure 1: Thermal Dissipation Probe for measuring sap flux velocity (Source (left): <http://labquipasia.blogspot.com/2010/05/report-on-workshop.html> and right (author))

Heat Field Deformation (HFD) method is applied to larger trees with thicker sap wood to measure high to low and also reverse sap flow (Fernandez, 2011; ICT International, 2011a) and is based on the analysis of temperature differences around a linear heater inserted in the sapwood. The HDF technique is a thermodynamic method based on measuring the temperature difference of the sapwood both axially and tangentially using two pairs of differential thermocouple around a line heater (Fig 2.2). An elliptical heat field under zero flow condition is achieved by continuously heating the linear heater at approximately 90 mA. The measured temperature difference applied in Equation 2 is used to calculate sap flux density.



Figure 2: Heat Field Deformation for measuring Sap flux density (Source: <http://www.ictinternational.com.au/hfd.htm>)

$$J_s = 3600D \frac{K + dT_{\text{sys}} - dT_{\text{as}}}{dT_{\text{as}}} \cdot \frac{Z_{\text{ax}}}{Z_{\text{tg}}} \quad 2$$

Where,  $J_s$  is the sap flux density in  $\text{g cm}^{-1} \text{h}^{-1}$ ,  $dT_{\text{sys}}$  and  $dT_{\text{as}}$  are the temperature differences recorded by the axial thermocouple junctions and tangential thermocouple junctions respectively,  $Z_{\text{ax}}$  is the axial distance between any end of the symmetrical thermocouple and the heater (taken as 1.5 cm),  $Z_{\text{tg}}$  is the tangential distance between the upper end of the asymmetrical thermocouple and the heater (taken as 0.5 cm),  $D$  is the thermal diffusivity of the fresh wood (taken as  $0.0025 \text{ cm}^2\text{s}^{-1}$ ) and  $K$  is the difference between  $dT_{\text{sym}}$  and  $dT_{\text{as}}$  under zero flow condition. The HFD method is used to obtain the radial profile of sap flux density (Nadezhdina *et al.*, 2002a) in thick trees with large sapwood depth.

### 2.3.3. Measurement of sap wood area

The transport of water from the root to the plant stem occurs through the active sapwood also known as xylem (Schurr, 1998). The accurate measurement of the xylem area is very important for the accuracy of the tree transpiration mapping (Bieker and Rust, 2010; Gebauer *et al.*, 2008; Rust, 1999). The extent of the active xylem area varies with tree species; therefore the selection of appropriate method is also important.

The most common and inexpensive method of determining sapwood is by staining the heartwood with reagents like benzidine (Rust, 1999). In this method, the reagent is prepared by mixing aqueous solutions of benzidine (5 gm) in hydrochloric acid (25 gm) and water (1 litre) and sodium nitrite (1 litre). The reagent dyes the heartwood dark red and the sapwood yellow (Rust, 1999). Resistance to penetration is another method that uses 1.8 mm diameter needle rotating at 15000 rpm dragging into the wood. The higher water content in sapwood provides higher resistance for the needle to penetrate and the power needed to penetrate it gives the measure of the conductive sapwood and heartwood (Rust, 1999). Computer Tomography is a non-destructive method of estimating sapwood depth which measures the attenuation of a collimated beam of radiation from several direction, which increases with increasing density and moisture (Rust, 1999) and considered to be more accurate method of sapwood depth estimation (Bieker and Rust, 2010).

### 2.3.4. Upscaling sap flow measurement

The total transpiration at the plot level is determined by the sum of total water uptake by the trees divided by the plot area. According to Lubczynski (2009), the upscaling of tree transpiration involves an upscaling scalar (stem basal area or canopy area), an upscaled parameter (sap flux density or sap wood area), a biometric upscaling function (BUF) and an upscaling technique. The stem area is usually considered to be better upscaling scalar than the canopy area but needs intensive work. However, availability of the high resolution remote sensing data may ease the upscaling method using canopy area.

The BUF can be developed between the sapwood area with the stem area or canopy area with sampling of the trees. However, the application of canopy area will be dependent on the availability of the high resolution image; otherwise stem area can be considered. Selection of sampling strategy and scaling methods are also equally important (Granier *et al.*, 1996; Smith and Allen, 1996). For the upscaling parameter, combining temporal variability of species and age based sap flux density with constant sapwood area can give better result (Lubczynski, 2009). The plot level transpiration depends on the tree densities, species available, soil properties and climatic condition (Lubczynski, 2000). The evaluation of the up scaled tree level transpiration with independent method of transpiration is rare (Ford *et al.*, 2007; Fregoso, 2002; Kumagai *et al.*, 2005) and the up scaling becomes more complicated when the study area has more tree species of different age.

## 2.4. Rainfall interception

The total amount of rainfall intercepted, stored and later lost by evaporation is considered to be a canopy interception loss. Interception loss is an important component of water balance in the tropical rain forest (Crockford and Richardson, 2000; Pereira *et al.*, 2009) and play a significant role in the overall catchment yield. Interception loss can vary from 10-20% in hardwood to 20-40% in conifers (Rutter *et al.*, 1972). However, it is not good to draw the conclusion for a particular forest type as interception loss is the function of rainfall type and other meteorological conditions during the study period (Crockford and Richardson, 2000). Crockford and Richardson (2000) elaborated the forest type properties as canopy storage capacity, leaf area index, leaf angle and cover, the storage capacity of shrub and litter layers, water repellence capacity of leaf and wood, projecting trees crowns and site conditions like aspects and exposure to wind and the meteorological factors as amount, intensity and duration of rainfall, wind speed and wind direction and air temperature and humidity. Therefore, it is necessary to identify, quantify and take into account the factors influencing the interception loss.

There are many studies carried out to model the interception loss. The estimation of ET by conventional water budget method in forest is prone to errors due to ungauged subterranean transfers of water into or out of the catchment (Schellekens, 2000) and thus needs above canopy meteorological observation and continuous measurement of throughfall for higher precision.

The studies carried out based on the measurement of rainfall, throughfall and stem flow have shown high correlation between the interception loss and the gross rainfall (Clarke, 1986/87) and thus a linear regression equation was developed between gross rainfall and interception.

The recommendation by Helvey and Patric (1965) to use one regression equation for summer and other for the winter was criticized by Jackson (1975) for not considering the rainfall intensity, duration and interval between events. The physically based computer model developed by Rutter *et al.* (1971) obtained wide acceptance in the interception loss modelling but complex computer programming makes this model time consuming to construct and operate (Gash., 1979).

Gash. (1979) developed a simple analytical rainfall interception loss model to simplify the Rutter model with the primary assumption of representing the real rainfall pattern by a series of discrete storms with sufficient interval for the canopy to dry. The model has been successfully applied in different canopy covers by Gash *et al.* (1980), Pearce and Rowe (1981), Bruijnzeel *et al.* (1987), Dolman (1987), Lloyd *et al.* (1988) and Hutjes *et al.* (1990). An important assumption made by Gash. (1979) is that the ratio of mean evaporation rate to the mean rainfall rate is constant and these values derived from several storms are representative for rest of the individual storms. The model was revised by Gash. *et al.* (1995).

The Gash model consists of five components: a) evaporation from small storms, b) during wetting up canopy, c) from the saturated canopy until rainfall ceases, d) after the rainfall ceases and e) evaporation from the trunks. The terminology and equations used in the model are presented in Table 2.1 and Table 2.2. The rainfall necessary to saturate the canopy is estimated by:

$$P_G' = -\frac{\bar{R}S_c}{\bar{E}_c} \ln\left[1 - \frac{\bar{E}_c}{\bar{R}}\right] \quad 3$$

Table 1: Terminology used in Gash Interception Model

Name	Definition	Symbol Used
Gross Rainfall	Rainfall measured in the open area closed to the study area or above the forest canopy	$P_G$
Threshold Rainfall	The threshold rainfall necessary to saturate the canopy	$P'_G$
Throughfall coefficient	Proportion of incident rainfall which falls directly to the forest floor without hitting the canopy	$p$
Stemflow coefficient	Proportion of the incident rainfall diverted to the trunks as stemflow	$pt$
Canopy cover	The percentage of the area influenced by the plants	$c$
Canopy capacity	The amount of water left on the saturated canopy when the rainfall and throughfall have ceased	$S$
Unit canopy capacity	It is the canopy capacity per unit area of the cover	$S_c$
Mean evaporation rate	Mean evaporation rate per ground	$\bar{E}$
Mean rainfall rate	Mean rainfall rate from the saturated canopy	$\bar{R}$
	Mean evaporation rate from the canopy	$\bar{E}_c$
	Trunk storage capacity	$St$

The accurate measurement of the rainfall (P), throughfall and stem flow is very critical as the underestimation of P or overestimation of TF or SF can give negative interception loss as reported by Valente *et al.* (1997). The rain gauges placed closed to the canopy can overestimate rainfall measurement due to the water blown from the canopy or underestimate in high intensity rainfall where large droplets have tendency to be blown away from collector (Crockford and Richardson, 2000). However, many studies hasn't highlighted the precise position of rain gauge, measurement of rainfall at an open location close to the forest is a usual practice. Similarly, throughfall can be measured by randomly located plastic gauges or rain gauges (Helvey and Patric, 1965) or large plastic sheet as net rainfall collector (Calder and Rosier, 1976). The former methods require a large number of plastic gauge and difficult to site the random position of the gauges (Calder and Rosier, 1976) whereas the later method is not practical for long term measurement as trees have to be watered regularly as no water reaches the ground after the plastic is placed (Crockford and Richardson, 2000). For the collection of stem flow split plastic hose is wrapped around the tree and attached with galvanized iron staples then sealed with neutral silicone sealant and connected to standard measuring bucket-gauges (Silva and Okumura, 1996). Since, stem flow contribution to the interception loss is very small, little attention has been paid to it (Crockford and Richardson, 2000).

Table 2: The original and revised analytical Gash Model equations (Gash. *et al.*, 1995)

Component of the Interception Model	The Original Gash (1979) model	Revised Analytical Model
For the small storm insufficient to saturate the canopy (no of storm = m)	$(1 - p - p_t) \sum_{j=1}^m P_{G,j}$	$c \sum_{j=1}^m P_{G,j}$
Evaporation from wetting up the canopy ( $P'G < PG$ ) (no of storm = n)	$n(1 - p - p_t)P'_G - nS$	$ncP'_G - ncS_c$
Evaporation from the saturated canopy	$\frac{\bar{E}}{\bar{R}} \sum_{j=1}^n (P_{G,j} - P'_G)$	$\frac{c\bar{E}_c}{\bar{R}} \sum_{j=1}^n (P_{G,j} - P'_G)$
Evaporation after the rainfall ceases	$nS$	$ncS_c$
Evaporation from trunk (q storms which saturate and truck and n+m-q storm which do not)	$qS_t + P_t \sum_{j=1}^{m+n-q} P_{G,j}$	$qS_c + P_t \sum_{j=1}^{n-q} P_{G,j}$

## 2.5. Evaporation from degraded land

The unsaturated zone play a significant role in the hydrological cycle through infiltration, soil moisture storage, evaporation, plant water uptake, ground water recharge and runoff (Simunek *et al.*, 2009). The ET in the bare soil equals to the bare soil evaporation that comes from unsaturated zone soil moisture profile. Water table is the most important factor affecting the soil evaporation, the more shallow the water table more water is available for evaporation (Stormount and Coonrod, 2004) and the other factors governing the soil evaporation are the climate, surface cover and soil properties. Bare soil evaporates at the potential rate during some days after rainfall and it continuously decreases after rainfall due to drying of the soil surface (Stroosnijder, 1987). Most of the method reviewed in the section 2.2 can be used to estimate the soil evaporation. Besides these methods, continuously monitoring the soil moisture profile can also be done to estimate the evaporation from the depleted moisture (Stroosnijder, 1987). The soil moisture derived from the microwave remote sensing is another promising methods to evaluate the spatial distribution of the evaporation in the soil (Chanzy and Bruckler, 1993).

There are two approaches discussed by Chanzy and Bruckler (1993) for the use of soil moisture to estimate soil evaporation. The first approaches consider soil surface moisture as the top boundary condition and take into account the hydraulic conductivity or diffusivity changes between the surface layer and deeper layers as water continuously evaporated from the soil. The second approach relates the soil resistance that limits the vapour flow from the soil surface. However, accurate measurement of the resistance to water vapour movement is the main limitation of the approach (Qiu *et al.*, 1998).

The conventional method of modelling unsaturated zone considering the uniform flow is not promising from the recent studies which demonstrated the existence of non-equilibrium water flow (Šimůnek and van Genuchten, 2008). However, the introduction of numerical modelling through various software packages has solved the problem of complexity introduced due to non-uniform flow consideration. The commonly used software packages listed by University of California (2012) are STANMOD, HYDRUS, VLEACH, VS2DI, VSAFT2, R-UNSAT, Johnson and Ettinger Models, SUTRA, TOUGH2, ParFLOW and STOMP. All of these software package are available free. Some of these and other additional software are also listed by Simunek *et al.* (2008).

## 2.6. Surface Energy Balance System:

Remote sensing technique with high spatial resolution is a useful tool for the assessment of energy balance to estimate evapotranspiration (Courault *et al.*, 2005). The surface energy balance equation (SEBS) proposed by Su (2002) is used for the estimation of atmospheric turbulent fluxes and evaporative fraction using satellite earth observation data, in combination with meteorological information at proper scales.

The main principal involved in the model is the energy balance equation which can be written as:

$$R_n = G_o + H + \lambda E \quad 4$$

Where,  $R_n$  is the net radiation,  $G_o$  is the soil heat flux,  $H$  is the sensible heat flux and  $\lambda E$  is the latent heat flux.

The net radiation ( $R_n$ ) is calculated by:

$$R_n = (1 - \alpha) \cdot R_{swd} + \varepsilon \cdot R_{lwd} - \varepsilon \cdot \sigma \cdot T_0^4 \quad 5$$

Where  $\alpha$  is the albedo,  $\varepsilon$  is the emissivity,  $R_{swd}$  is the downward solar radiation,  $R_{lwd}$  downward long wave radiation,  $\sigma$  is the Stefan-Boltzmann constant, and  $T_0$  is the surface temperature.

The soil heat flux ( $G_o$ ) will be calculated as:

$$G = R_n [\Gamma_c + (1 - f_c) \cdot (\Gamma_s - \Gamma_c)] \quad 6$$

For full vegetation cover,  $\Gamma_c = 0.05$  (Monteith. and Unsworth, 2008) and  $\Gamma_c = 0.315$  for bare soil (Kustas and Daughtry, 1990)

The sensible heat flux is the most difficult component of the energy balance to determine. It is calculated on the basis of following equation with continuous iterations.

$$H = \rho_a \cdot c_p \cdot (T_s - T_a) / r_{ah}$$

where  $\rho_a$  is specific mass density,  $c_p$  is specific heat,  $T_s$  is land surface temperature,  $T_a$  is air temperature and  $r_{ah}$  aerodynamic resistance. The aerodynamic resistance is calculated on the basis of following equations:

$$\left[ -\frac{k \cdot (z - d_o)}{w' \theta_0'} \cdot \frac{d\bar{\theta}}{dz} = \phi_h(\xi) \Rightarrow \frac{d\bar{\theta}}{dz} = -\frac{\overline{w' \theta_0'}}{k \cdot (z - d_o)} \cdot \phi_h(\xi) \right] \quad 7$$

$$r_{ah} = \frac{1}{k \cdot u_*} \cdot \left[ \ln \left( \frac{z - d_o}{z_{oh}} \right) - \Psi_h \left( \frac{z - d_o}{L} \right) + \Psi_h \left( \frac{z_{oh}}{L} \right) \right] \quad 8$$

$$\theta_s - \bar{\theta} = \frac{H}{k \cdot u_* \cdot \rho \cdot c_p} \cdot \left[ \ln \left( \frac{z - d_o}{z_{oh}} \right) - \Psi_h \left( \frac{z - d_o}{L} \right) + \Psi_h \left( \frac{z_{oh}}{L} \right) \right] \quad 9$$

The instantaneous evapotranspiration will be converted to daily ET by using evaporative fraction (EF).

$$EF = \frac{\lambda E}{(R_n - G)} = \frac{\lambda E}{(\lambda E + H)} \quad 10$$

## 3. THE STUDY AREA

### 3.1. Location

Nepal is a topographically diverse area stretching 885 km east-west and 193 north-south direction with elevation from 90 m from the sea level to the peak of the world the Mt. Everest. The geography is generally divided into permanently snow covered high Himalayan, High Mountain, Middle mountain, Siwalik and Terai as shown in Fig 3. The middle mountain of Nepal occupies 30% of area providing livings for 45% of the total population. The elevation ranges from 800-2400 amsl.

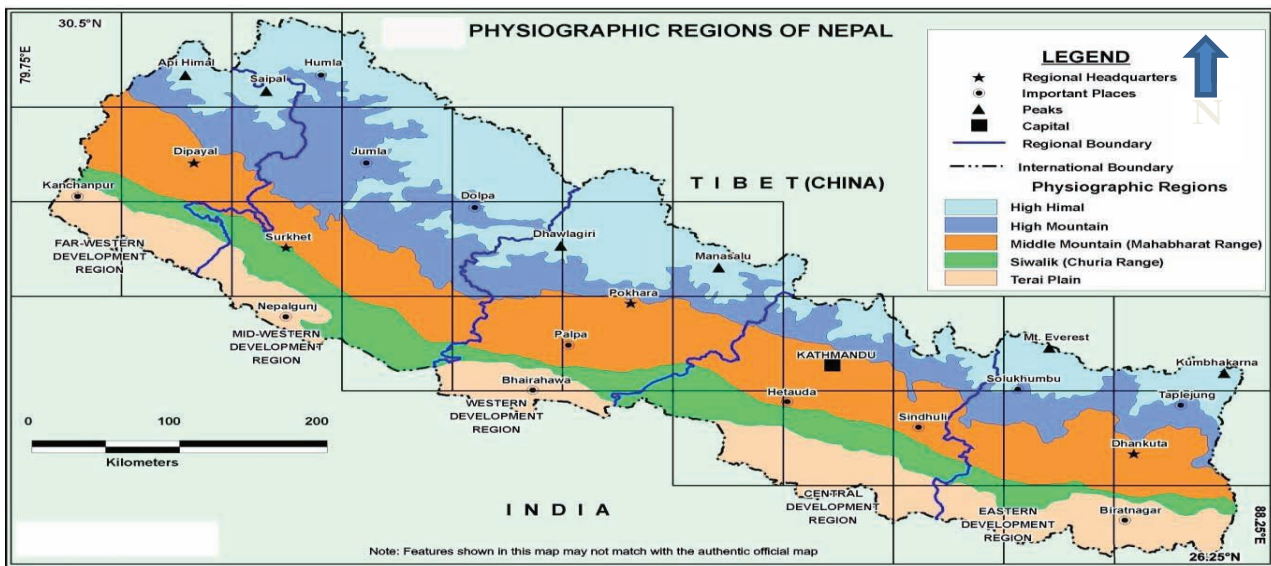


Figure 3: Physiographic regions of Nepal

Jhiku-Khola catchment selected for the present study is located in the middle mountain of Nepal where reforestation was carried out with the pine trees in the degraded pasture land and existing natural forest is mainly dominated by *Castanopsis tribuloides*. The detailed of the catchment area is documented by Merz (2004). The area is located in the Kavrepalanchowk district of the country and is about 45 km east from the capital city, Kathmandu. It lies between latitudes  $27^{\circ}35' N$  and  $27^{\circ}41' N$  and longitude  $85^{\circ}32' E$  and  $85^{\circ}41' E$  with the elevation from 800 m to 2020 m.

The total catchment area of the study area is 111 km<sup>2</sup>. The general aspect of the catchment is southeast, extending from southeast to northwest. The only highway connecting the country with China called Araniko Highway passes through the catchment. The location map of the study is shown in Fig 4 with three stands selected for study to represent the pine forest, natural forest and degraded soil. The details of the three locations are presented in Table 3.

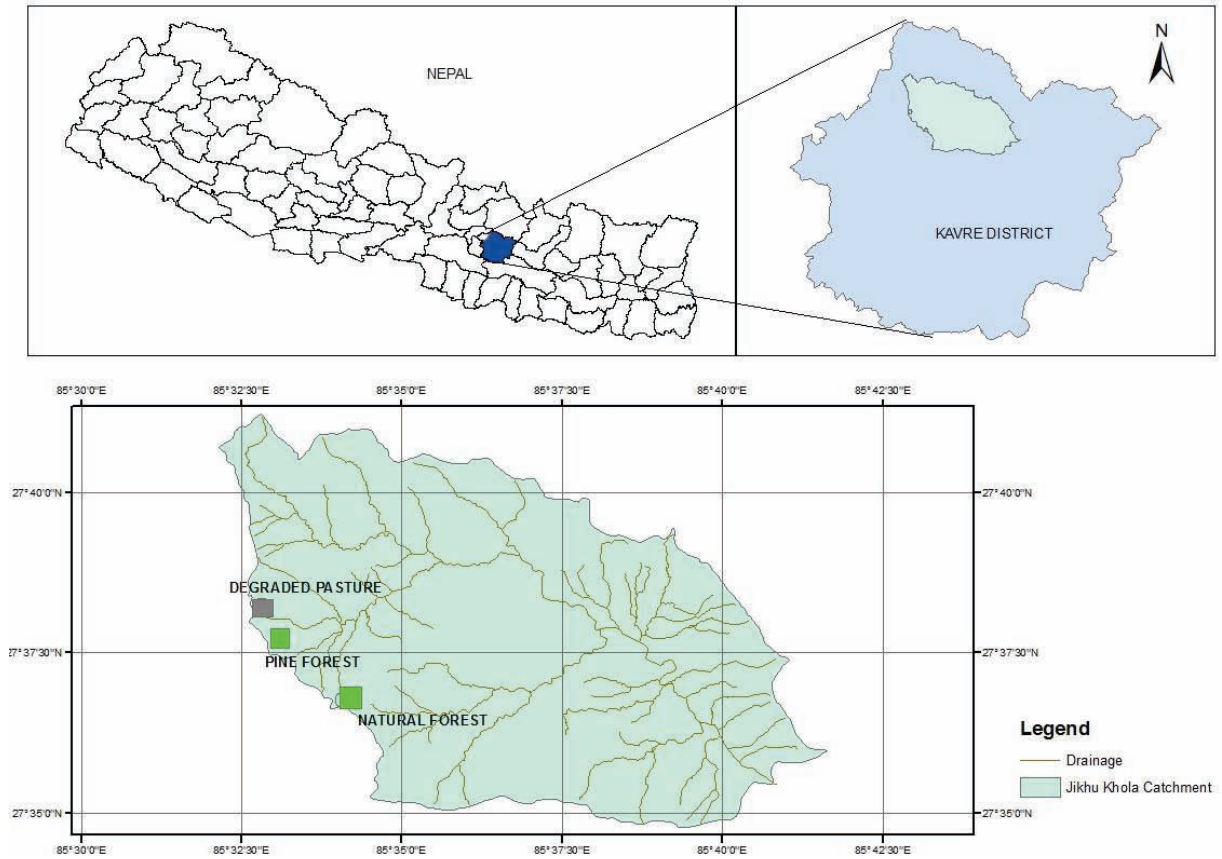


Figure 4: Location map of the study area

Table 3: Site information of the three stands

	Degraded Pasture	Pine Forest (PFS)	Natural Forest (NFS)
Elevation	1684 m	1424 m	1563 m
Co-ordinate	27° 38' 00" N, 85° 32' 30" E	27° 37' 00" N, 85° 34' 30" E	27° 36' 00" N, 85° 34' 30" E
Aspect	South-East (SE)	South-West (SW)	North-West (SW)
Slope	18°	20°	20°
Soil Texture	Silt loam	Silt loam	Silt loam
Forest Type		Evergreen	Evergreen
Size of plot		272 m <sup>2</sup>	225 m <sup>2</sup>
Tree density		625 trees/ha	1160 trees/ha

### 3.2. Land use and land cover

The Middle Mountain of Nepal is a densely populated area with intensive cultivation. The area is characterized by complex topography, climate, geology and vegetation. The land cover of the Jhikukhola

catchment is mostly dominated by the rain fed agricultural land and forest. Vegetation cover in the catchment is 30% forest land, 7% shrub land and 6% grass land with remaining 57% under agriculture. The watershed has a very active reforestation program supported by Australian Government.



Figure 5: Location of Degraded Pasture (Top left), Pine forest stand (Top right) and Natural forest stand (bottom)

### 3.3. Climate and hydrology

The climate of Jhikukhola watershed varies from humid sub-tropical to warm temperate. The long term mean annual rainfall ( $\pm$ SD) in Jikhu Khola catchment measured at Panchkhal (853 masl) in the period 1976 to 2000 was  $1226 \pm 200$  mm (Merz, 2004). The Middle Mountain of Nepal gets the major rainfall (80% of the total) from early June to the end of the September which is considered to be the monsoon season. The other seasons experienced are pre monsoon (March-May), post monsoon (October-November) and winter (December-February). The catchment has a total drainage length of 737.2 km with the drainage density of  $6.6 \text{ km/km}^2$  (Merz, 2004). The average temperature of the area is  $19.6 \text{ }^\circ\text{C}$  with the average maximum and minimum temperature of  $34.4^\circ\text{C}$  and  $3.74^\circ\text{C}$  respectively. The average Humidity varies from 55% in March to 95% in September and average monthly wind speed is always less than 2 m/s with slight seasonal variation (Merz, 2004).

## 4. METHODOLOGY

The annual transpiration from the Pine Forest Stand (PFS) and Natural Forest Stand (NFS) were calculated from the measurement of sap flux density and biometric properties of the trees. Again, the annual interception loss from both stands was estimated by using the analytical Gash interception model. The interception loss and sap flow were combined to obtain the stand level ET in the PFS and NFS. Similarly, one-dimensional HYDRUS model was used to obtain the degraded soil evaporation. The temporal variation of ET based on dry and wet season and spatial variation based on the land cover was finally assessed to see how reforestation affects the annual ET. Evapotranspiration using remote sensing data was also estimated based on SEBS algorithm to compare with the combined interception and transpiration measurement approach. The general methodology is presented in Fig 6 and each section is briefly explained below. However, the flowchart for the SEBS algorithm is presented in Fig 12.

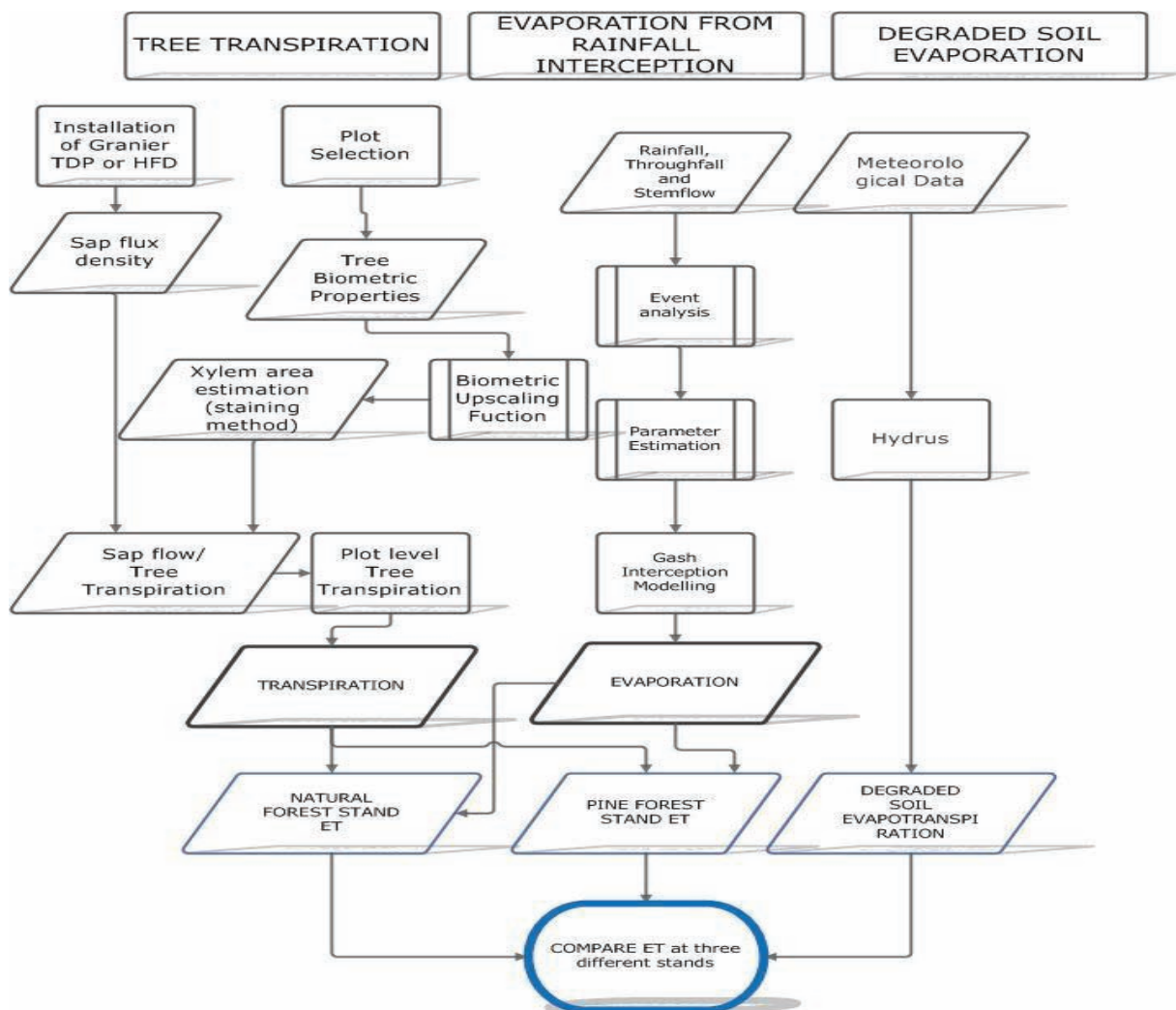


Figure 6: Flowchart of the methodology

#### 4.1. Data collection

Most of the data for the present study were obtained from C. P. Ghimire, Ph D (herein after referred to as collected data) student in Department of Water Resource, ITC while some of the data were collected during the field work in September, 2011. The data collected and measured during field work are listed in Table 4. The methods applied and instrumentation for the collection is briefly explained below.

Table 4: Data collected and measured

Data	Source
Sap flux density monitoring <ul style="list-style-type: none"> <li>• Long term monitoring (TDP)</li> <li>• Spatial distribution of sap flux density</li> <li>• Radial monitoring</li> <li>• NTG, Radial and Circumferential variation Monitoring</li> </ul>	Collected Collected Collected Measured
• Tree Biometric properties	Collected and Measured
Rainfall, Throughfall and Stem flow	Collected
Soil moisture content and bulk density	Collected
Meteorological data (Solar radiation, air temperature, humidity and wind speed)	Collected
Leaf Area Index	Measured

#### 4.2. Sap flux density and biometric parameters

The data for long term monitoring of sap flux density were collected in nine and six trees from the natural and pine forest respectively. The measurements were made from July 2010 to March 2011 at recording interval of 5 minutes. This data was used for the long term estimate of sap flux density in the two forest stands. Similarly, the data from a sap flow campaign from March to May, 2011 in four different locations in pine forest was also collected. These data were analysed to understand the spatial variability of sap flux density within the study area. A total of 48 pine trees were monitored using TDP sensors. The tree density, height of trees, diameter at breast height (DBH), and canopy projection area were measured from both the stands during the field campaign in September, 2011. Similarly, Leaf Area Index (LAI) was measured using LI-COR 2000 plant canopy analyser.

For the monitoring of NTG, the sensors were protected from the effect of direct solar radiation as shown in Fig 7. The sensors were covered by protective shields and then wrapped by aluminium foils. The data quality and the conditions of the sensors in the trees were regularly checked. Considering the fact that the pine forest is comparatively sparse as compared to the Natural forest, more measurements were taken in the PFS. In pine forest, the seasonal and spatial variability was monitored from the measurement in three different locations in dry season (during March-May Campaign) and one location in wet season (during September campaign). For the Natural trees, it was monitored during May, 2011 for six days within the stand.



Figure 7: Thermal insulation provided in the sensors for preventing from NTG

The radial variation of the sap flux density was monitored using HFD in the six pine trees in the stand, 5 collected from Campaign in March-May and one measured in September, 2011. The measurements were taken from 2-5 days. Similarly, the radial variation was measured in one dominant species in the natural forest stand. The radial profile of the sap flux density was analysed by the sap flow tool (ICT International, 2011b). A clear sky day average sap flux density of the measured tree was plotted against the sapwood depth and the profile was fitted with appropriate mathematical equation. The equation was used to integrate the 2 cm TDP measurement to whole sapwood depth and corresponding correction factor was developed to obtain the radially corrected sap flow.

The Circumferential Variability (CV) of sap flux density was observed in three pine trees of DBH 36.61 cm, 23.24 cm and 35.01 cm during the campaign in September, 2011. The sap flux density was monitored in four directions using TDP. Similarly, one pine tree of DBH 28.65 was selected for axial variation placing the sensors at 1.5 m apart axially during September. Measurements were taken for two days. As DBH in natural forest stand is very small, typically between 10-15 cm, no correction for circumferential and axial variability was envisaged (Lu *et al.*, 2004).



Figure 8: A cross section of a pine tree (left) and *Castanopsis tribuloides* (right) showing sapwood, heartwood and bark (Source: Ghimire, C, Personal Communication)

Almost whole sapwood in pine tree is conducting water (Rust, 1999) and also can be seen in the Fig 8. Staining of heartwood with Benzidine was used for xylem area estimation due to economic and simplicity in use (Rust, 1999). However, in case of natural forest Methyl orange solution was used as Benzidine solution doesn't dyes the sapwood distinctly. The method was made less destructive by comprehending the tree boring with the use of pressler borer as shown in Fig 9 instead of cutting the whole tree. A simple mathematical equation was used to calculate the area of the sapwood in which the heartwood area and bark area can be subtracted from the total stem area of the tree.



Figure 9: Tree boring for sapwood area determination (left) and obtain sample (right)

For the long term monitoring of the sap flux density, the missing sap flux density was extrapolated by the method proposed by Cienciala *et al.* (2000). In this method, the sap flux density is coupled with the climatic variable and extrapolated using the following equation:

$$J_s = \frac{a * R_s}{c + R_s} * (100 - b * RH) \quad 11$$

Where,  $J_s$  is a sap flux density ( $\text{cm}^3\text{cm}^{-2}\text{hr}^{-1}$ ),  $R_s$  is the incoming solar radiation ( $\text{kWm}^{-2}$ ) and RH is the relative humidity and a, b and c are the parameters. The parameters were calibrated and validated for given species and for each dry and wet season of the study period.

A strong correlation between the stem area and the sapwood area in pine and the dominant tree in natural forest was found. Thus this correlation function (BUF) was used to obtain the sapwood area of rest of the trees in the stands. The PFS consists of only one species. Therefore, a single regression analysis was done between the stem area and sapwood area and corresponding BUF was developed. However, the NFS consists of 5 species. The species *Castanopsis tribuloides* was the dominant species with 13 trees followed by *Schima wallachi* (4), *Quercus lamellosa*(3), *Myrica esculenta* (3) and *Rhododendron arboretum* (3). The BUF was developed in case of the dominant species *Castanopsis tribuloides* only while for the other a simple linear interpolation technique was used. The relationship between the sap flux density and sapwood area was derived in pine forest. In case of the natural tree average sap flux density was used. These functions were used to obtain the sap flow of the trees at the plot level. The plot level transpiration was obtained from the sum of the sap flow of the trees in the plot divided by the plot area.

### 4.3. Gash analytical model

The revised analytical Rainfall Interception model by Gash. *et al.* (1995) was used to estimate the evaporation from rainfall interception ( $I$ ) as the difference of rainfall and Throughfall. Event based analysis was carried out. Rain event is defined as the event with at least 0.4 mm of rainfall. The events were separated by at least three hours for the complete drying up the canopy (Schellekens *et al.*, 1999).

#### 4.3.1. Rainfall, throughfall and stem flow

The gross rainfall ( $P_G$ ) was collected from June 2010 to September 2011; whereas throughfall and stem flow were measured in the rainy seasons of 2011. As all these data were collected; detailed instrumentation is not presented here. The obtained rainfall distribution is shown in Fig 10. The natural forest stand (NFS) and pine forest stand (PFS) receives a total rainfall of 1418 mm and 1506 mm respectively. A total of 73% and 77% rainfall occurs between June-September in the two stands respectively whereas inclusion of May constitute more than 85% in both the stands. This justifies the rainfall pattern and separation of the dry (June-September) and wet season (October-June) by Merz (2004).

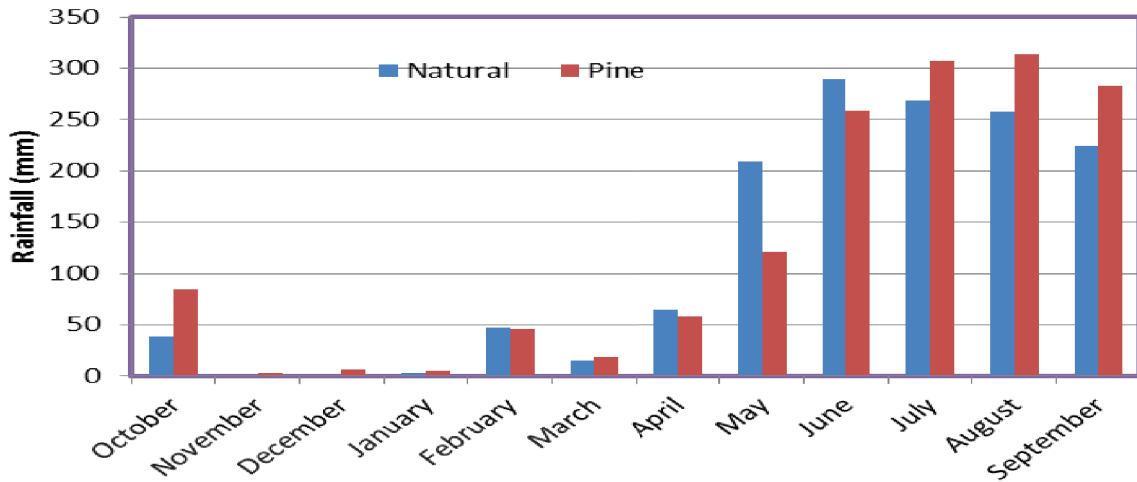


Figure 10: Rainfall distribution in NFS and PFS

#### 4.3.2. Model application

The parameters used for the rainfall interception model are canopy storage capacity ( $S$ , mm), free throughfall coefficient ( $p$ ), trunk water capacity ( $S_t$ , mm), the proportion of rain diverted to the stem flow ( $p_t$ ) and ratio of mean wet canopy evaporation ( $\bar{E}$ ,  $\text{mmhr}^{-1}$ ) assumed to occur when  $P > 0.5 \text{ mmhr}^{-1}$  (Gash., 1979) to mean rainfall rate ( $\bar{R}$ ,  $\text{mmhr}^{-1}$ ). The canopy cover ( $\phi$ ) in the Gash Model is estimated as  $1-p$ . As the calibration and validation of the model was carried out by Ghimire *et al.* (2012) during the rainy season of 2011, the calibrated parameters were used to obtain the interception loss for rest of the period. However, the methods used for model parameter estimation are described here briefly.

The canopy parameters ( $S$  and  $p$ ) were derived using the method of Jackson (1975) from the regression line of scatter plot of gross rainfall and throughfall. The graph gives the increase of throughfall with gross rainfall at a fairly constant rate and then shows a steepening slope. Rutter *et al.* (1972) assumes that the first envelops represents the attainment of canopy saturation and the second envelop represents the variation of evaporation from wet canopy. The throughfall after the steepening of the graph can be represented by:

Throughfall ( $TF$ ) = Gross Rainfall ( $P_G$ ) – Canopy Saturation Value ( $S$ )

Therefore, a line of unit slope with x-axis and negative intercept on y-axis gives the value of  $S$ . Similarly, the coefficient of throughfall ( $p$ ) was determined as the slope of regression between  $R$  and  $TF$  for storms that are too small to fill the canopy storage (Jackson, 1975) considering that the evaporation losses during these storms are negligible. The stemflow parameters  $St$  and  $pt$  were derived from the method of Gash and Morton (1978) as the negative intercept and slope of linear regression line between stem flow and gross rainfall. The graph developed by Ghimire *et al.* (2012) for parameter estimation in pine forest is shown in Fig 11.

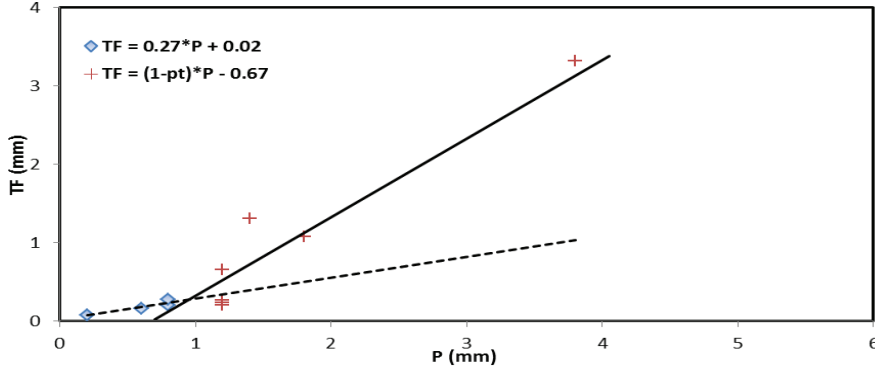


Figure 11: Estimation of canopy parameters  $S$  and  $p$  using the method of Jackson (1975) for pine forest (Ghimire *et al.*, 2012)

The mean wet canopy evaporation ( $\bar{E}$ ) from the forest canopy was derived from the linear regression of  $P_G$  and  $TF$ . The value of  $\bar{E}$  was also determined by the method by Monteith (1965) considering the resistance factor zero. A final estimate of  $\bar{E}$  was obtained from the optimization procedure where  $\bar{E}$  was adjusted to minimize the root mean square error (RMSE) and difference between the modelled and measured interception loss.

#### 4.4. Evaporation from degraded pasture land

The one dimensional HYDRUS-1D model is a simple model to simulate one dimensional movement of water, heat and solute in unsaturated zone. It is also low cost, requires low memory and have good visualization (Simunek *et al.*, 2008). The model uses linear finite elements to numerically solve the Richard's equation which is expressed as:

$$\frac{\partial \theta}{\partial t} = \frac{\partial}{\partial z} \left( K \frac{\partial h}{\partial z} + K \right) - S \quad 12$$

Where,  $\Theta$  is the water content [ $L^3L^{-3}$ ],  $t$  is time [ $T$ ],  $z$  is the vertical co-ordinate positive upward ( $L$ ),  $h$  is the pressure head [ $L$ ],  $K$  is the unsaturated hydraulic conductivity [ $LT^{-1}$ ] and  $S$  is the source or sink [ $T^{-1}$ ].

The unsaturated hydraulic property is described by van Genuchten model which is expressed as:

$$\frac{\theta - \theta_r}{\theta_s - \theta_r} = \left[ \frac{1}{1 + (ah)^n} \right]^m \quad 13$$

Where,  $\Theta$  is the soil water content [ $L^3L^{-3}$ ],  $\Theta_r$  is the residual soil water content [ $L^3L^{-3}$ ],  $\Theta_s$  is the saturated soil moisture content [ $L^3L^{-3}$ ],  $h$  is the pressure head [ $L$ ],  $m$  is the parameter called shape parameter and  $n=1/(m-1)$ .

HYDRUS was used to calculate the evaporation from the degraded pasture land. It calculates the evaporation considering the factor affecting fluxes such as precipitation, infiltration, surface runoff, soil moisture storage, hydraulic conductivities and specific water capacities (Deme, 2011). The model estimates the transpiration from the water uptake by the plant root. However, in the degraded pasture condition, the soil surface is bare, so the ET is attributable to evaporation component only, which is obtained from the change in the soil moisture level in the soil profile. The model was run on the daily basis. Laboratory analysis of soil sample carried out in the soil lab of ITC to obtain the textural class. For the textural analysis, the gravel fraction of the soil sample was sieved off, rinsed with demi water, dried at 40°C and weighted. First the sand was separated with a 50  $\mu$ m sieve and the clay and silt were determined by pipette method.

The model was run from September 2010 to December 2010 for calibration. Model was calibrated with the measured average soil moisture content in the profile based on the initial guess of the model parameter. The boundary condition was set as atmospheric boundary with surface layer at upper boundary condition and the free drainage at the lower boundary condition. The upper boundary condition permits the water to build up on the surface from precipitation and the lower boundary condition was selected because the ground water level is very deep in the present study area. The initial condition was the soil moisture content in the soil profile on the first day of simulation. The calibration was done for  $\Theta_r$ ,  $\Theta_s$ , alpha and  $K_s$ .

#### 4.5. Evapotranspiration from SEBS

Landsat Enhanced Thematic Mapper plus (ETM+7) was selected for the purpose as it has better spatial resolution and are freely available. The temporal resolution of Landsat is 16 days so a total of 48 data can be available for the study period. Cloud free data for the wet season was not available so two days during the dry season was selected. For this, the bands of Landsat 7 on passing day of November 2, 2010 and February 22, 2011 were used.

Landsat 7 ETM+ sensor is an eight band multi spectral scanning radiometer, seven spectral at spatial resolution of 30 m and one panchromatic with spatial resolution of 15 m. The swath width is 183 km. The band information is provided in Table 5.

Table 5: Landsat ETM+ bands

Band Number	wavelength region	wavelength ( $\mu$ m)	Resolution (m)
1	VIS	0.45-0.515	30
2	VIS	0.525-0.605	30
3	VIS	0.63-0.69	30
4	NIR	0.75-0.90	30
5	SWIR	1.55-1.75	30
6	TIR	10.4-12.5	30
7	SWIR	2.09-2.35	30
8	PAN	0.52-0.9	15

Pre-processing of the images was done in ENVI. The DN values in the thermal bands were converted to radiance and for other bands it was converted to reflectance. These bands were used to obtain the inputs for the SEBS. The SEBS algorithms use five land surface parameters. These parameters are land surface temperature, emissivity, albedo, NDVI and fraction of vegetation cover and all these were derived from the bands of Landsat. Air pressure, temperature, humidity and wind speed at the reference height was obtained from the meteorological measurement. DEM was made from the contour of 20 m obtained from Department of survey, Nepal.

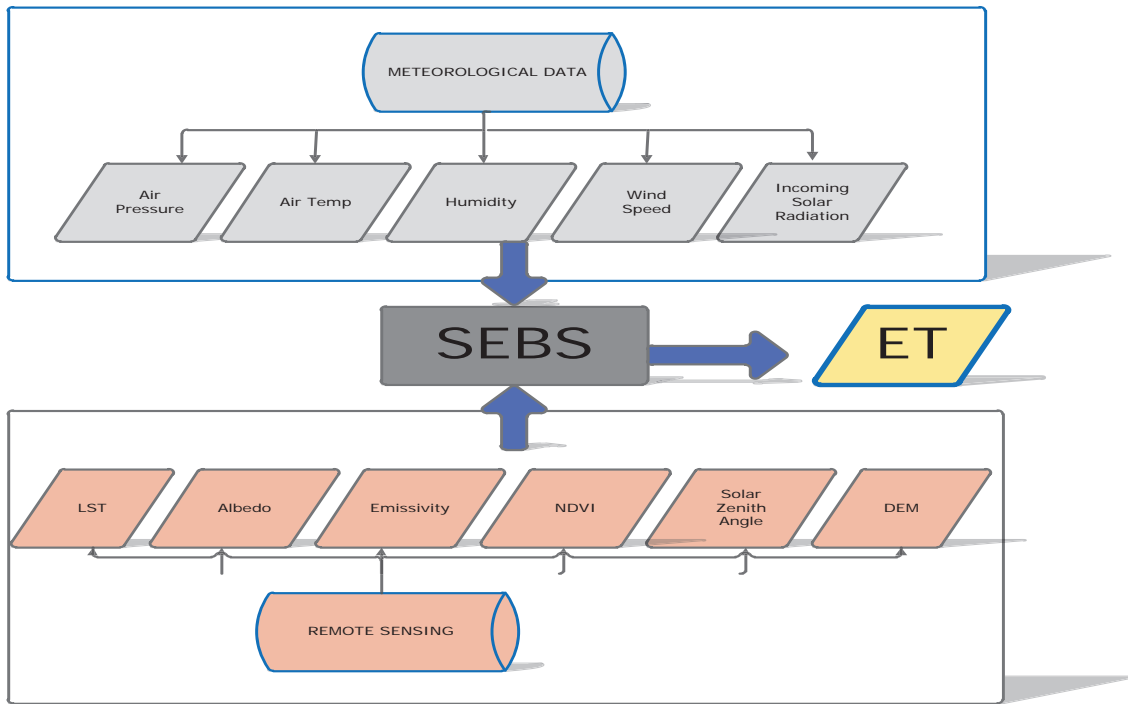


Figure 12: Methodology applied for SEBS

### Land Surface Temperature:

The thermal band 61 was used to derive the land surface temperature using the following equation:

$$T = \frac{K2}{\ln\left(\frac{K1}{L} + 1\right)} \quad 14$$

Where, T is the land surface temperature (K), K1 and K2 are calibration constants ( $W/(m^2sr\mu m)$ ) equal to 666.09 and 1282.71 respectively and L is the radiance of thermal band.

### NDVI:

The NDVI was estimated from the reflectance of the red and near infrared band. In Landsat band 3 and band 4 are these bands. So the NDVI is derived as:

$$NDVI = \frac{\rho4 - \rho3}{\rho4 + \rho3} \quad 15$$

Where  $\rho4$  and  $\rho3$  are the reflectance in the near infrared and red bands respectively.

**Fractional vegetation cover (Fc):**

The fractional vegetation cover was estimated from NDVI as:

$$Fc = (NDVI - NDVI_{min})^2 / (NDVI_{max} - NDVI_{min})^2 \quad 16$$

Where  $NDVI_{max}$  and  $NDVI_{min}$  values were assigned as 0.5 and 0.2 respectively obtained from the help file of the SEBS algorithm in ILWIS.

**Emissivity:**

The emissivity was estimated as proposed by Valor and Caselles (1996):

$$\epsilon_0 = \epsilon_c Fc + \epsilon_s (1 - Fc) + 4 * \langle d\epsilon \rangle Fc * (1 - Fc) \quad 17$$

Where  $\epsilon_c$  is the emissivity of the full vegetation cover,  $\epsilon_s$  is the emissivity of bare soil,  $Fc$  is the fractional vegetation cover and  $\langle d\epsilon \rangle$  vegetation structure parameter. The value of  $\epsilon_c$ ,  $\epsilon_s$  and  $\langle d\epsilon \rangle$  were taken as 0.985, 0.96 and 0.015 respectively.

**Albedo:**

The land surface albedo was estimated from reflectance band 2, band 4 and band 7 applying the following equation developed by Shunlin (2001).

$$ALBEDO = 0.526 * \rho_2 + 0.3139 * \rho_4 + 0.112 * \rho_7 \quad 18$$

Where,  $\rho_2$ ,  $\rho_4$  and  $\rho_7$  reflectance from band 2, band 4 and band 7 respectively.

**4.6. Standard meteorological data**

The meteorological data like solar radiation, wind speed, relative humidity and air temperature were collected at 3 m height above the ground level from June, 2010 to September, 2011. Wind speed and incoming solar radiation were measured using A100R switching anemometer and SKS110 Pyranometer respectively. The temperature and humidity was measured using Vaisala HMP45C probe. All the measurements were taken at 5-minutes interval in Campbell Scientific Ltd CR23X logger. The daily average solar radiation, relative humidity, wind speed and minimum and maximum are shown in Fig 13.

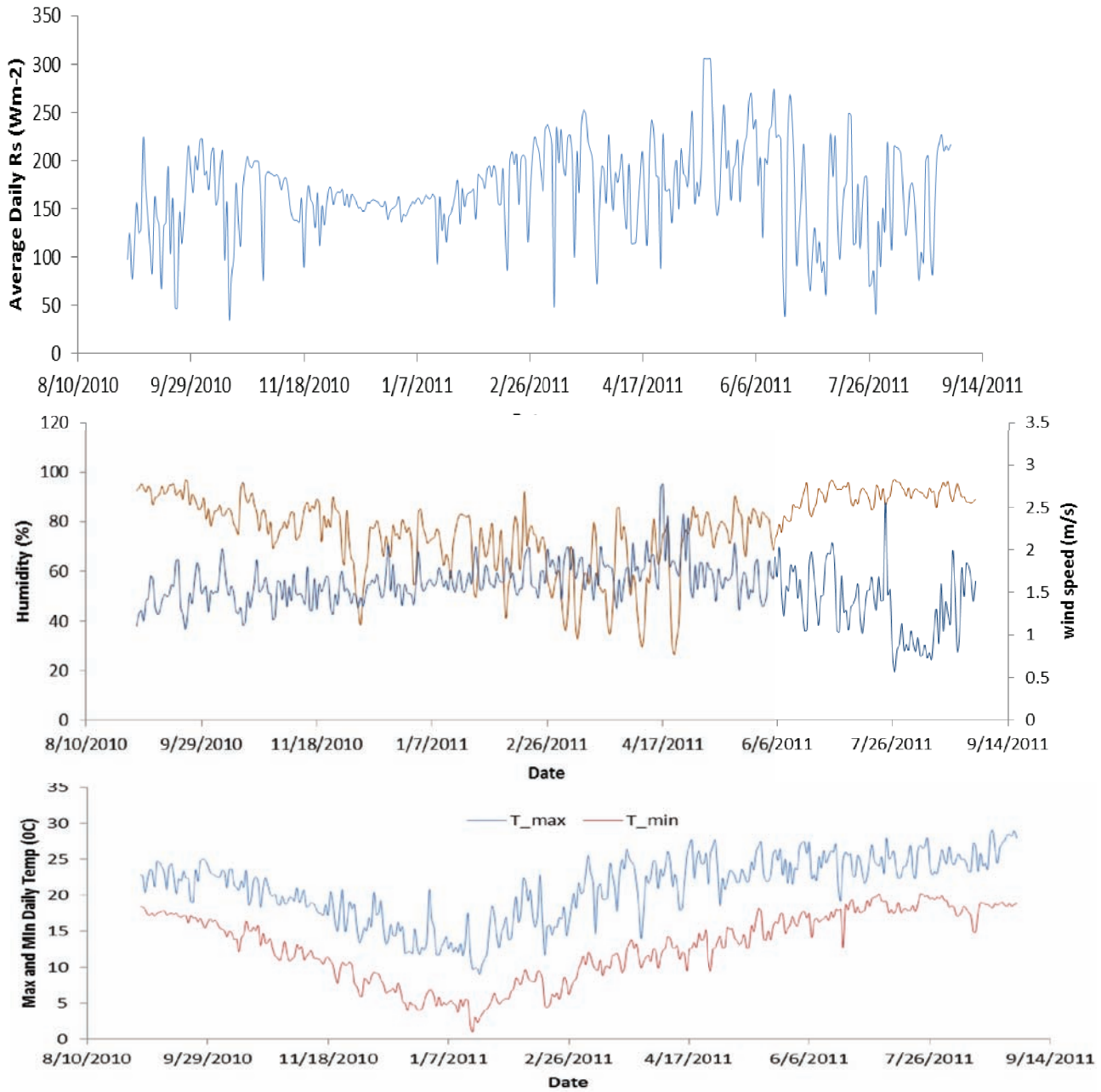


Figure 13: Daily average solar radiation, relative humidity, and wind speed and maximum and minimum temperature measured in the study area from September, 2010 to August, 2011

## 5. RESULTS

### 5.1. Rainfall interception

#### 5.1.1. Model application

The Gash model was calibrated and validated by Ghimire *et al.* (2012) splitting the measured rainfall and throughfall into two groups of events in both stands. The calibration and validation were carried out from the rainfall events of the wet season of 2011. The model parameters derived by Ghimire *et al.* (2012) are listed in the Table 6. These parameters were applied to obtain the interception loss for rest of the period.

Table 6: Parameters of the revised Gash Model derived by Ghimire *et al.* (2012) in the study area

Parameter	NFS	PFS
$S$ (mm)	0.89	0.67
$S_c$ (mm)	1.1	0.92
$P'_c$ (mm)	1.21	1
$p$	0.19	0.27
$c$	0.81	0.73
$St$ (mm)	0.02	0.033
$pt$ (mm)	0.017	0.007
$st/pt$	1.18	4.71
$\bar{R}$ (mmhr <sup>-1</sup> )	1.73	2.43
$\bar{E}_c/R$	0.179	0.16
$\bar{E}$ (mmhr <sup>-1</sup> )	0.25	0.29

#### 5.1.2. Rainfall interception by NFS and PFS

The total annual interception loss in NFS and PFS were 323 mm and 276 mm respectively and represented 23% and 19% of the total annual rainfall. The daily evaporation from the NFS during wet and dry seasons was 1.95 mm and 0.35 mm respectively and that of the PFS was 1.70 mm and 0.28 mm respectively. The higher interception loss in NFS is as expected as due to high density forest with high leaf area index. The LAI of PFS and NFS measured in September, 2011 were 2.21 and 5.23 respectively.

Table 7: Total Interception loss in two stands, in mm

Season	NFS			PFS		
	Rainfall	$I$	% $I$	Rainfall	$I$	% $I$
Wet Season	1032.97	238.39	23.08	1168.65	207.19	17.73
Dry Season	368.50	84.59	22.96	313.34	68.89	21.99
Total	1401.47	322.98	23.05	1481.99	276.08	18.63

Since, for the event analysis only the rainfall above 0.4 mm was considered, the total rainfall from the events in Table 7 is lower than the rainfall presented in section 4.3.1. The rainfall out of the events are less than 2%, thus it is considered that the error associated with this is insignificant.

The major contributor of the evaporation from the interception loss are the evaporation from the saturated canopy and after rainfall ceases and both contributed about 90% of the total loss in both stands. Stem flow has the lowest contribution (less than 1.5%), thus is neglected in most of the interception loss studies.

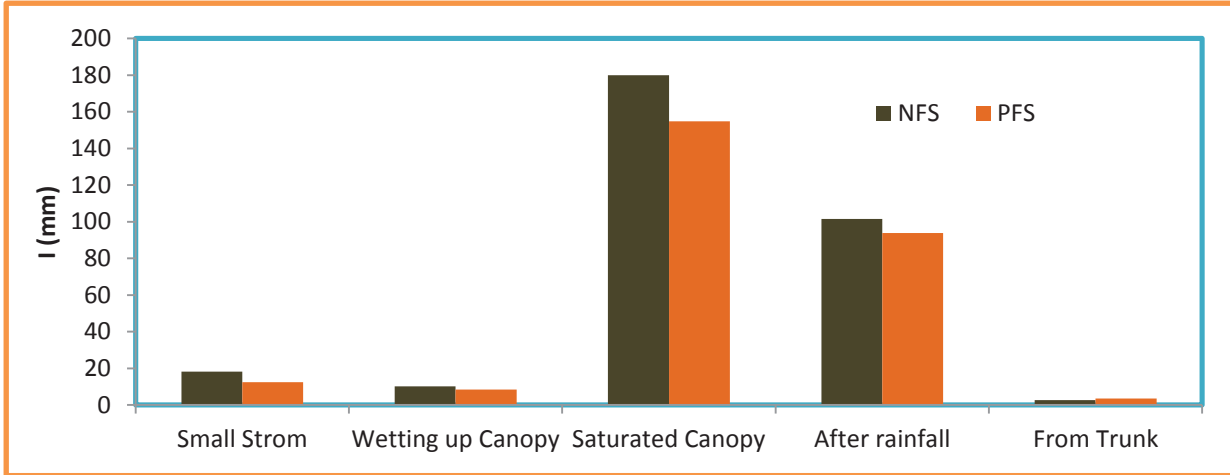


Figure 14: Contribution of components of Gash model to total interception loss

The sensitivity analysis was carried out from the set of events used for the calibration of the model in both stands. The sensitivity analysis was done by increasing and decreasing the model parameters by 10% and respective TF and RMSE were observed and are presented in Table 8.

The sensitivity analysis shows that the determination of  $\frac{\bar{E}}{\bar{R}}$  is very important as it is more sensitive than the other parameters. This is due to the fact that the major contributor of the interception loss comes from the saturated canopy, as shown in Figure 14, where this ratio plays a crucial role.

Table 8: Sensitivity analysis model parameters in Gash model

		Original		+10%		-10%		% change (+)	%change (-)	
		TF	RMSE	TF	RMSE	TF	RMSE	TF	TF	
PFS	Original									
	$\bar{E}/\bar{R}$	0.12	372.89	2.08	366.62	2.16	375.93	2.05	-1.68	0.82
	$S$	0.67	372.89	2.08	370.77	2.08	374.5	2.08	-0.542	0.459
	$p$	0.27	372.89	2.08	374.77	2.06	370.76	2.1	0.531	-0.545
NFS										
	$\bar{E}/\bar{R}$	0.145	366.74	1.58	360.04	1.53	373.58	1.67	-1.83	1.87
	$S$	0.89	366.74	1.58	364.24	1.57	369.34	1.58	-0.68	0.71
	$p$	0.19	366.74	1.58	367.15	1.58	366.44	1.58	0.11	-0.08

## 5.2. Stand level transpiration

### 5.2.1. Forest stand characteristics

The total numbers of trees with their species and DBH in the two forest stands are presented in Annex A. The trees used for the sap flux density monitoring and total number of the days used for the analysis are shown in Table 9. The NFS has the area of 225 m<sup>2</sup> whereas PFS has the area of 272 m<sup>2</sup> with 26 and 17 number of trees respectively. The size of the tree in the PFS is larger than the trees in the NFS. The average DBH( $\pm$ SD) of the pine tree was 26.64 $\pm$ 4.79 cm whereas that in natural tree was 12.08 $\pm$ 2.75 cm. The natural forest stand is mostly dominated by *Castanopsis tribuloides* followed by *Schima wallachi*, *Quercus lamellosa*, *Myrica esculenta* and *Rhododendron arboretum*.

Table 9: Biometric properties of trees monitored in PFS and NFS (values associated with dry and wet indicates the total number of trees used for the analysis in the wet and dry seasons)

Tree ID	DBH (cm)	Sapwood depth (cm)	selected no of days for analysis		Tree Species	
			Dry	Wet	Local	Botanic
PINE FOREST STAND (6-Dry, 6-Wet)						
Tree 1	31.8	13.75	31	25	Sallo	<i>Pinus roxburghii</i>
Tree 2	26.4	10.25	37	19	Sallo	<i>Pinus roxburghii</i>
Tree 3	22.3	8.5	14	14	Sallo	<i>Pinus roxburghii</i>
Tree 4	30.2	11	14	18	Sallo	<i>Pinus roxburghii</i>
Tree 5	31.2	8	11	17	Sallo	<i>Pinus roxburghii</i>
Tree 6	25.5	9.75		13	Sallo	<i>Pinus roxburghii</i>
Tree 7	19.7	8	14		Sallo	<i>Pinus roxburghii</i>
NATURAL FOREST STAND (12-Dry, 8-Wet)						
Tree 1	15.8	3.05	25	47	Musure Katus	<i>Castanopsis tribuloides</i>
Tree 2	12.4	4.95	24	47	Musure Katus	<i>Castanopsis tribuloides</i>
Tree 3	9.4	4.65	24	47	Falat	<i>Quercus lamellose</i>
Tree 4	12.7	3.4	23	47	Musure Katus	<i>Castanopsis tribuloides</i>
Tree 5	10.9	4.8	23	47	Musure Katus	<i>Castanopsis tribuloides</i>
Tree 6	15.5	5.8	23	47	Musure Katus	<i>Castanopsis tribuloides</i>
Tree 7	8.8	3.55	22		Falat	<i>Quercus lamellose</i>
Tree 8	13.8	6.05	25	15	Kafal	<i>Myrica esculenta</i>
Tree 9	10.4	4.15	14	37	Musure Katus	<i>Castanopsis tribuloides</i>
Tree 10	10.8	4.3	8		Lali Guras	<i>Rhododendron arboretum</i>
Tree 11	15.9	5	6		Falat	<i>Quercus lamellose</i>
Tree 12	12.7	3.05	6		Musure Katus	<i>Castanopsis tribuloides</i>

### 5.2.2. Sap flux density ( $J_s$ )

The sap flux density follows pattern similar to that of solar radiation. The three trees in Fig 15 shows a slight lag to the peak of the solar radiation however follow the similar pattern. It means that the sap flux density is maximum after the noon. However, the time to attain the peak may vary according to the position of the tree in the stand (McJannet *et al.*, 2007).

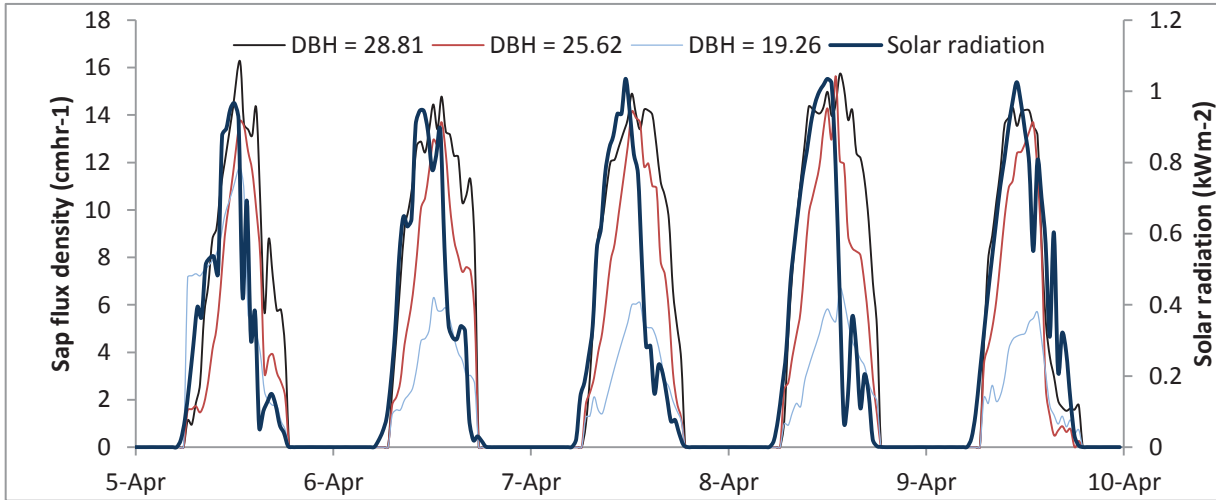


Figure 15: Sap flux density in three pine trees showing strong correlation with the incoming solar radiation

### 5.2.3. Natural Thermal Gradient (NTG)

The monitoring of the NTG was carried out both in the Natural and Pine forest stands considering the three points below.

- Good insulation for preventing the introduction of direct solar radiation into the sensor is necessary for preventing NTG (Lu *et al.*, 2004) (Fig 7)
- NTG has high spatial and seasonal variation (Do and Rocheteau, 2002b) thus three locations in pine forest and one location in natural forest was selected for monitoring. Two of the locations in pine forest was used during dry season and one for wet season.
- The temperature difference between the probes to be within  $\pm 0.2$  °C when the sensor is unpowered (Do and Rocheteau, 2002b)

NTG measured in the study are shown in Fig 16. It is evident from the figure that the NTG is generally within  $\pm 0.2$ °C and hence is within the threshold value proposed by Do and Rocheteau (2002b) with very few moments crossing 0.2 °C. Therefore, no correction for the NTG was envisaged.

### 5.2.4. Circumferential and axial variability of sap flux density

The result shows that the average sap flux density ( $J_s$ ) is higher in west direction while lower in the south. However, the difference is not significant as shown in Fig 16. The measurement of  $J_s$  was made in the North direction which seems to be more representative of the overall average in all directions; therefore, no correction for the circumferential variation was done. Similarly, the average  $J_s$  measured in axial distance of 1.5 m was 2.06 cmhr<sup>-1</sup>. The sap flux density at the bottom was slightly smaller than the top one. The measurement at the higher position of the tree has the opportunity of getting higher solar radiation which can introduce natural gradient giving higher value than the bottom. Therefore, the measurement was taken at the breast level.

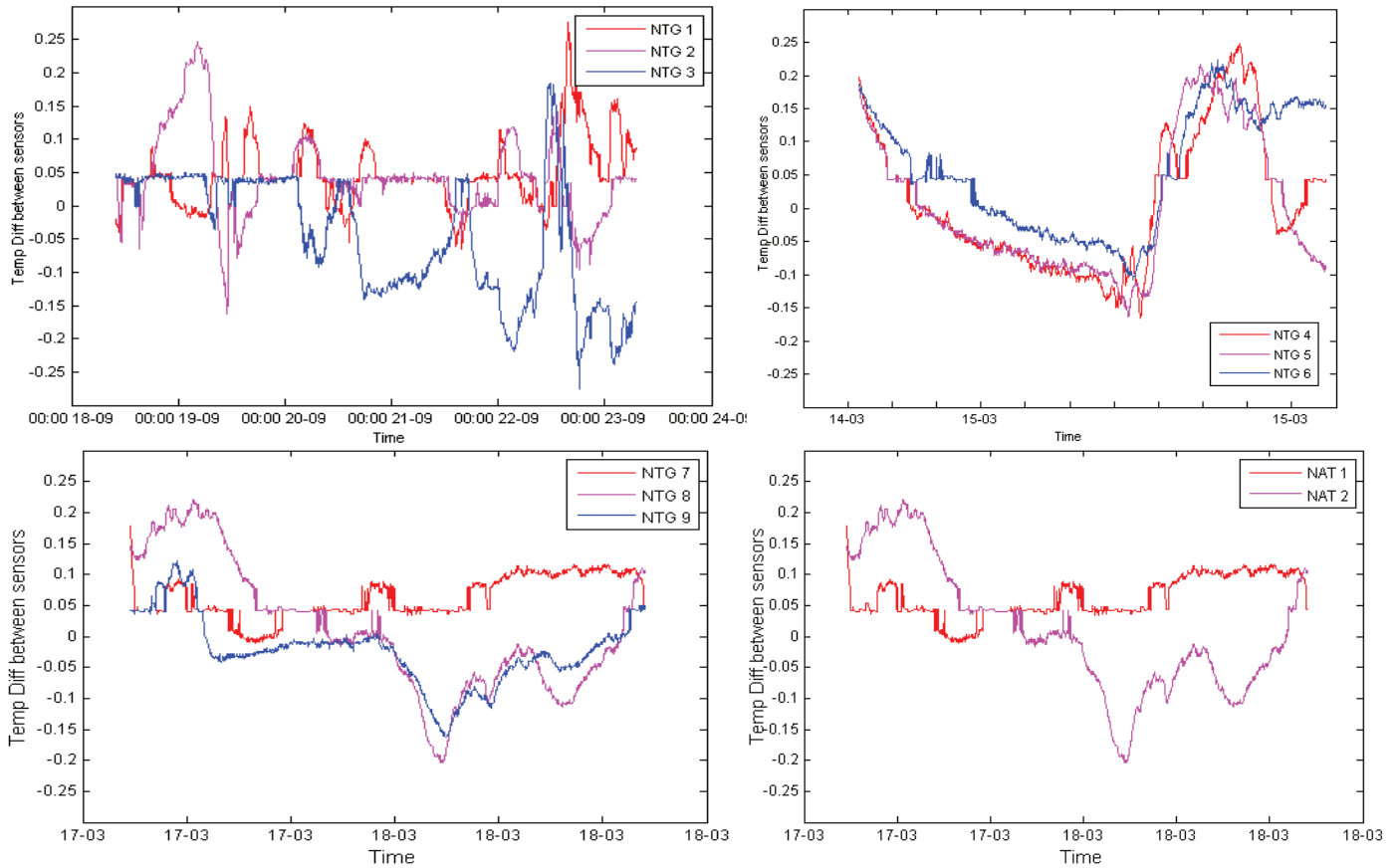


Figure 16: NTG Monitoring using unpowered TDP in three different locations of pine forest (Top and bottom left) and one location in natural forest (bottom right)

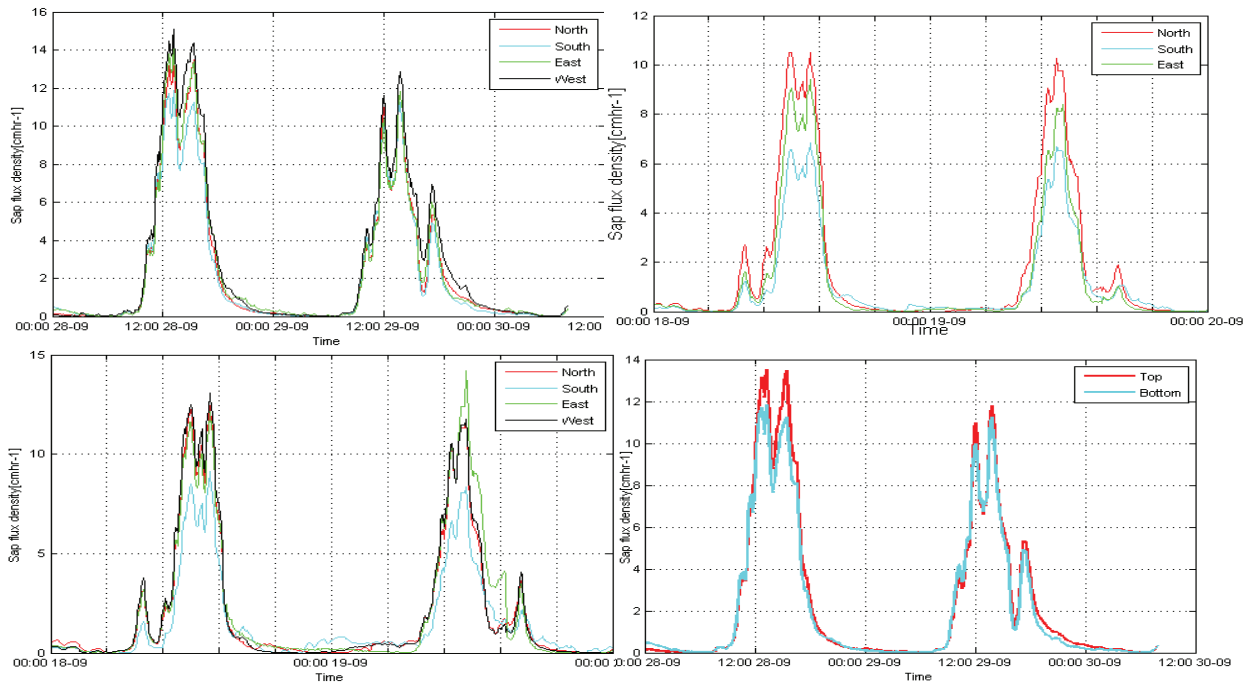


Figure 17: Circumferential (Top and bottom left) and axial (bottom right) variation of sap flux density in Pine trees monitored using TDP

Table 10: Average sap flux density in circumferential direction of pine trees

Tree ID	DBH (cm)	Date	Average Js (cmhr-1)				average
			North	South	East	West	
CV1	36.61	18-Sep	2.071	1.444	2.047	2.157	1.930
		19-Sep	1.878	1.532	2.137	1.916	1.866
CV2	23.24	18-Sep	1.885	1.145	1.480		
		19-Sep	1.601	1.050	1.126		
CV3	35.01	28-Sep	2.997	2.729	3.152	3.472	3.088
		29-Sep	2.320	2.177	2.299	2.816	2.403

### 5.2.5. Temporal extrapolation of sap flux density

The extrapolation of the Js was needed to estimate the total sap flow in the dry and wet season and this was done using the method proposed by Cienciala *et al.* (2000). This model was selected as it was developed under the similar humid climatic conditions as the present study area. Humid climatic condition was the main assumption of the model, considering sufficient water is available for tree transpiration. The method combine the non-linear response of Js with short wave radiation (Rs) and linear response to humidity (RH) and both of these inputs were available. The main reason for considering these two meteorological forcing is that the Js is highly correlated with these two meteorological forces. Therefore, the dependence of Js with RH and Rs was tested by calculating the Pearson correlation coefficient and is shown in the Table 11. Since the result shows a high correlation of Js with RH and Rs, the model can be applied in the present condition. The correlation was done selecting five days of measured sap flux density with half-hour average.

The calibration of the model for extrapolation of the sap flux density was done on the individual tree; the maximum numbers of the representative days for the respective tree were taken. Therefore the number of the representative days varied from 6 to 42 in NFS and 11 to 37 in the PFS as shown in Table 9 with the average of 19 and 22 days in PFS and NFS respectively.

Table 11: Pearson Correlation coefficient between Js and RH and Rs

	Season	Rs	RH
Pine	Dry	0.71	-0.83
	Wet	0.72	-0.83
Natural	Dry	0.90	-0.52
	Wet	0.89	-0.82

The average model parameters and the corresponding errors are presented in Table 12 whereas the values for each tree are shown in Annex B. The model gives satisfactory results but has a poor correlation for simulating the peaks. The ignorance of the wind speed, which has high influence on the tree transpiration, is probably the main drawback of the model. The calibrated and validated profiles of the sap flux density on selected trees on both seasons of the two stands are shown in Fig 18.

Table 12: Model parameters and associated errors in two seasons of both stands

Forest stand	Season	Parameters			Error			
		a	b	c	Calibration		Validation	
					RMSE (cmhr-1)	MAE (cmhr-1)	RMSE (cmhr-1)	MAE (cmhr-1)
PFS	Dry	0.289	0.860	1.273	1.16	0.58	1.84	0.84
	Wet	0.258	0.743	2.297	0.90	0.59	1.04	0.50
NFS	Dry	0.361	0.701	1.398	1.98	0.98	2.58	1.40
	Wet	0.677	0.885	1.027	1.38	0.71	1.63	0.84

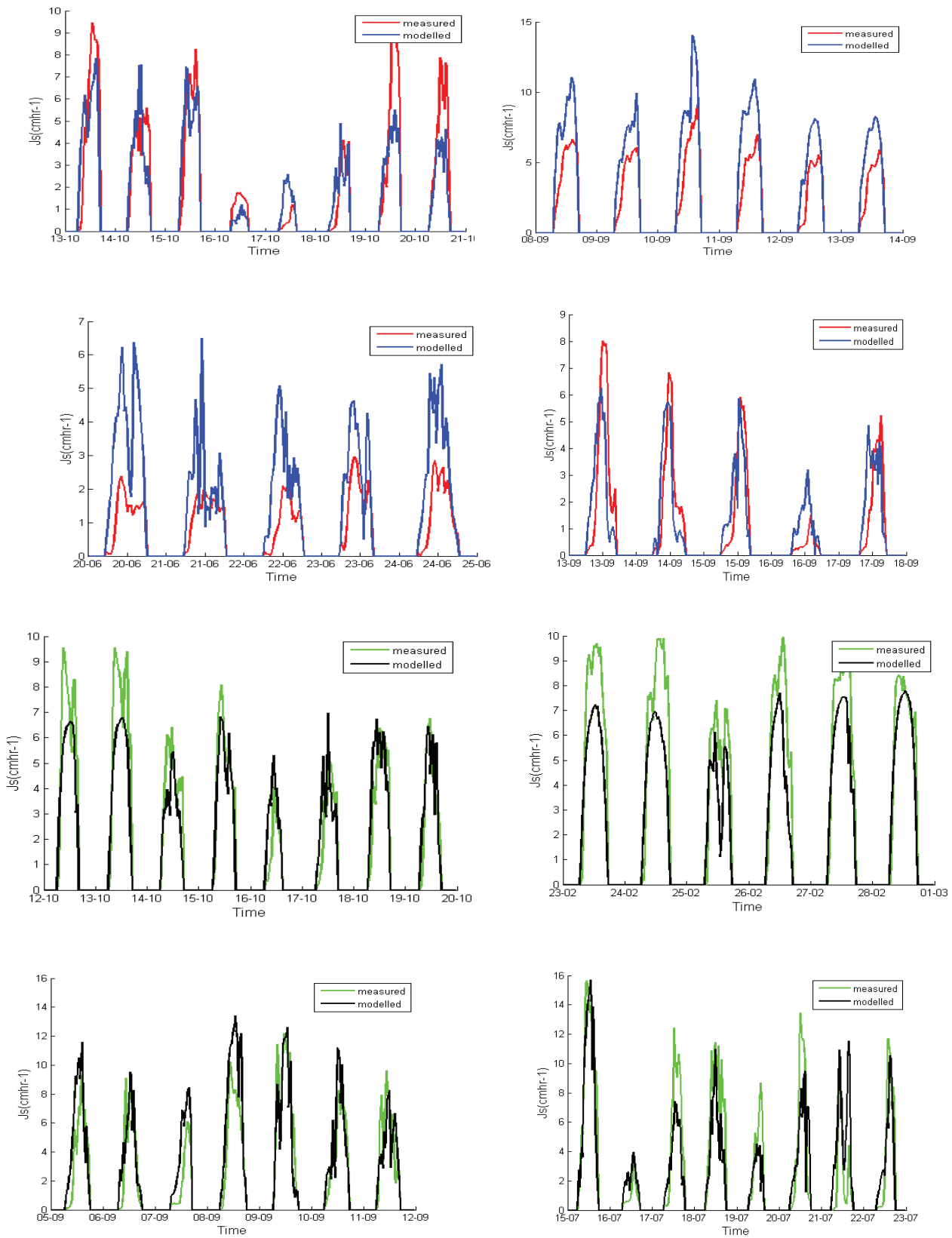


Figure 18: Sap flux density in Cienicala model calibration (left) and validation (right), starting from top to down pine tree in dry season, pine tree in wet season, natural tree in dry season and natural tree in wet season

**5.2.6. Upscaling of sap flow to stand level**

The relationship between tree stem area and sapwood area is shown in Fig 19 and the estimated sapwood area for the rest of the trees in the stands is shown in Annex A. The BUF developed for Pine and *Castanopsis tribuloides* are:

$A_x = 0.5214 * A_s + 16.568$	For Pine Trees	19
$A_x = 0.3971 * A_s + 30.963$	For <i>Castanopsis tribuloides</i>	20

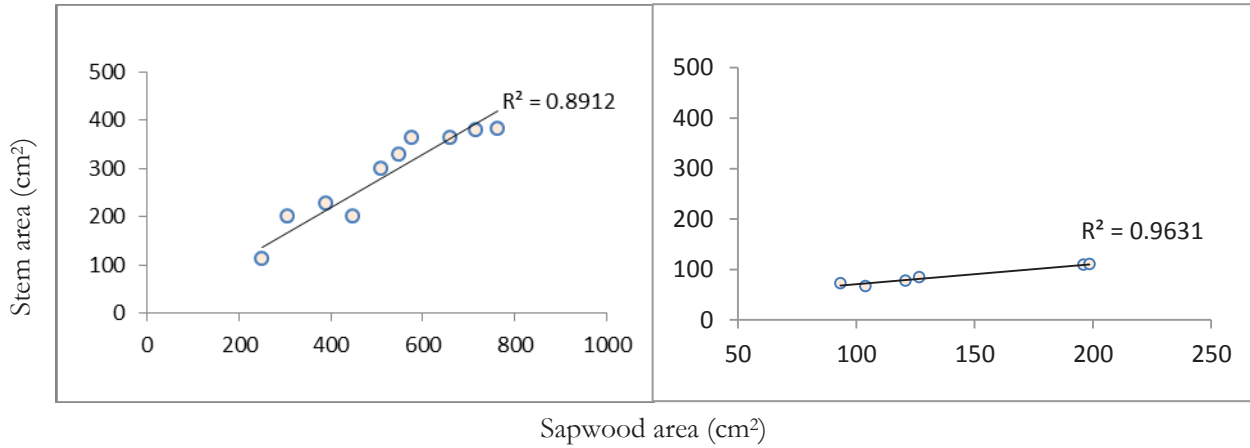


Figure 19: BUF for Pinus (left) and *Castanopsis tribuloides* (right) with a least square linear fit

The sap flux density in the PFS showed a strong correlation with the sapwood area as shown in Fig 20 with the higher  $J_s$  with high sapwood area. These correlations give the relationship shown in equation 21 and 22 during the dry and wet season respectively. Therefore, the relationships were applied to obtain the sap flux density for rest of the trees in the stand.

$J_s(pd) = 0.0099 * A_x$	$R^2 = 0.89$	21
$J_s(pw) = 0.0042 * A_x$	$R^2 = 0.89$	22

Where  $J_s(pd)$  and  $J_s(pw)$  are the sap flux density for the pine in dry and wet seasons respectively.

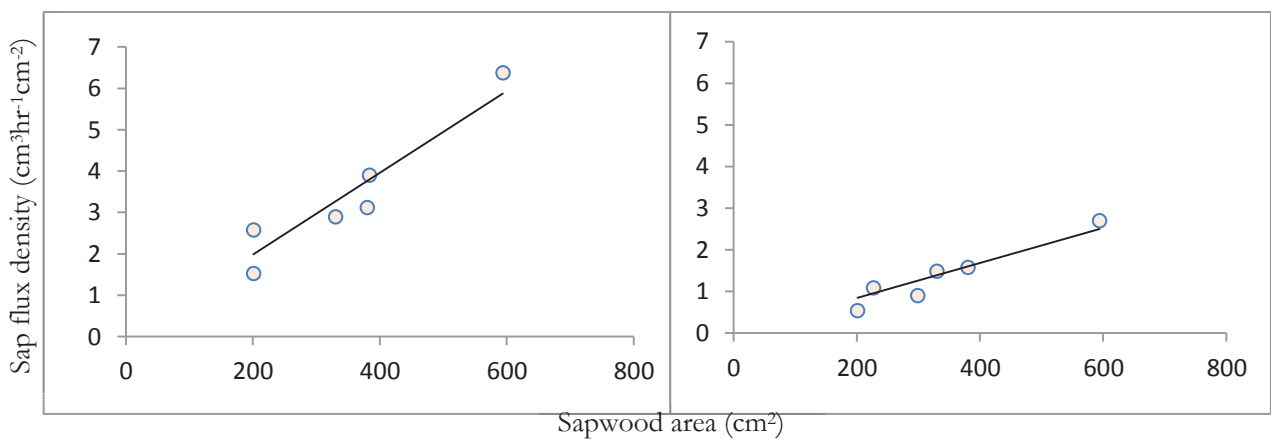


Figure 20: Relationship between sapwood area and sap flux density in the dry (left) and wet (right) seasons in the PFS

In case of the NFS, the sap flux density doesn't show any trends as compared to the pine trees as shown in Fig 21. However, in case of the dominant tree the sap flux density seems increasing with the increasing sapwood area and then decreasing following a second order polynomial function. But the correlation was not strong ( $R^2 = 0.57$  in wet,  $0.43$  in dry) therefore, average value was considered more appropriate.

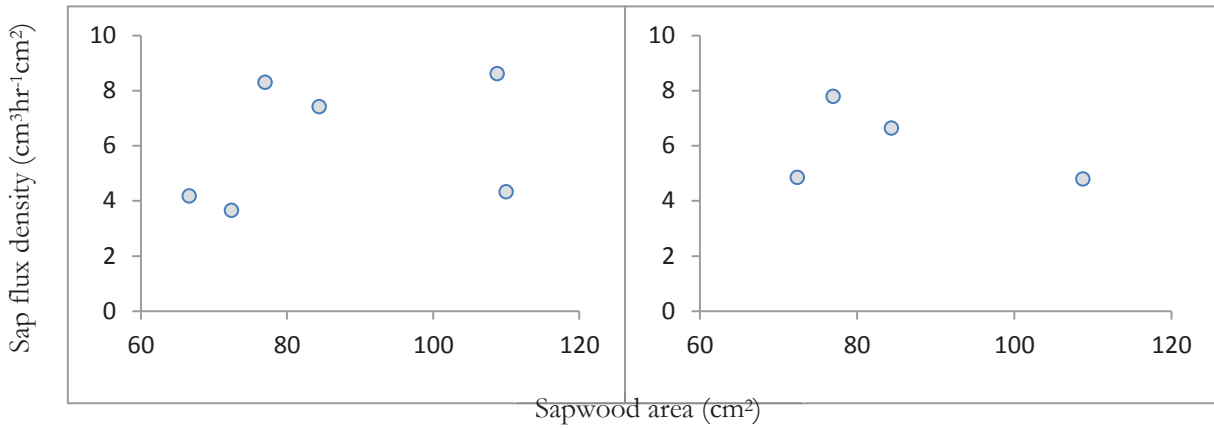


Figure 21: Relationship between sapwood area and sap flux density in the dry (left) and wet (right) seasons in *Castanopsis tribuloides* of the NFS

### 5.2.7. Radial variability of sap flux density

The radial profile shows that the sap flux density varies significantly with the depth. The radial profile in the *Pinus roxburghii* tree shows the sap flux density is high at the outer sapwood and decreases linearly with the sapwood depth. However, that profile doesn't represent the trend discovered by Ford. *et al.* (2004) in the *Pinus* family in Georgia where sap flux density first increased with depth but then decreased providing relation similar to the Gaussian function.  $J_s$  in the pine trees of the study area follow a linear profile, decreasing along the depth. This shows that the same pine family doesn't necessarily show the same radial profile, which varies with space and climate and therefore, introduction of literature based function to correct the radial profile can introduce uncertainties in sap flow calculation. Similarly, the radial profile developed for the dominant natural forest tree *Castanopsis tribuloides* shows that  $J_s$  drops sharply with depth, thus is represented by the exponential function. The profiles obtained from the five representative pine trees and one natural tree is shown in Fig 22 with the function representing the profile in equation 23 and 24.

$$J_{sp} = -0.17Y_x + 2.51 \quad R^2=0.95 \quad 23$$

$$J_{sn} = 2.372e^{-0.282Y_x} \quad R^2=0.95 \quad 24$$

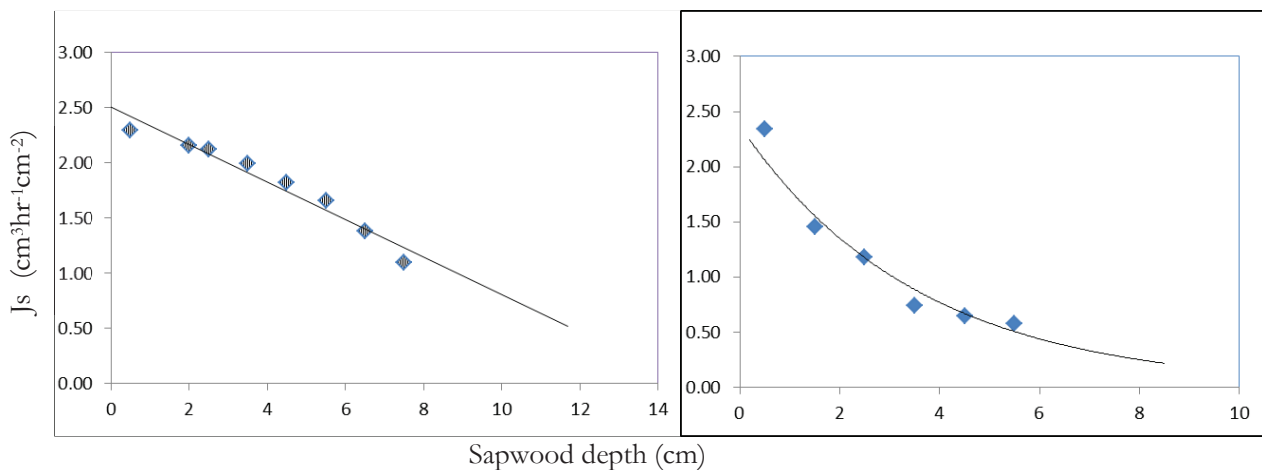


Figure 22: Radial profile of sap flux density in pine tree (left) and natural tree (right) obtained from HFD measurements

The radial variability of the  $J_s$  was measured by HFD, at eight different depths from 0.5 cm to 7.5 cm at every interval of 1 cm. Therefore, the first two measurements at 0.5 cm and 1.5 cm of the HFD can be

considered representative of the TDP measurement at 2 cm depth. The average sap wood depth of the trees monitored for the radial profile was 12.43 cm and for the natural tree it was 6.2 cm.

Table 13: Proportion of sap flux density integrated over the entire sap wood depth and depth of TDP measurement

Forest stand	Sap flow (cm <sup>3</sup> /hr)		Overestimation by ratio
	Considering the radial profile	TDP equivalent flow	
Pine	534.53	1084.63	2.03
Natural	97.74	229.45	2.35

The radially corrected sap flow can be obtained by integrating the functions as:

$$Q_s = \int_r^h 2\pi x f(x) dx \quad 25$$

Where, x is the sapwood depth, r and h are the radii of cambium and heartwood; f(x) is the function representing the radial profile of the tree. Equation 25 was integrated from 0 cm to 2 cm to obtain sap flow equivalent to TDP (standard length 2 cm) and then integrated from 0 cm to the average sapwood depth of the respective tree to obtain the total sap flow in the entire sapwood. The result shows that TDP referring to the outermost 2 cm of the Js profile typically overestimates the sap flow by two times in pine tree as shown in Table 13. That overestimation is even larger in the natural forest where Js is overestimated by 2.35 times, as natural trees show sharper exponential decrease in the sap flux density along the sapwood depth.

After estimating the TDP equivalent of HFD radially corrected flow, a correction factor was developed as the ratio of actual sap flow to the TDP equivalent flow. In order to apply the correction factor for the stands with different tree size compared to the tree monitored for HFD a single correction factor may not be representative, as the proportion varies when the same equation is integrated to different sapwood depth. The trees in the stands were divided into different groups with respect to the sapwood depth and correction factor for the respective groups was obtained using the average sapwood depth of the respective group. The trees in the PFS have higher range of sapwood depth (7.75 cm) compared to the trees in natural forest stand (3 cm), and therefore were divided into three groups and the natural trees were divided into two groups. The average sapwood depth of the trees in NFS was 4.52 cm so the trees were separated into the above average and below average groups. Similarly, the pine trees were divided into the trees above 12 cm, between 9 cm to 12 cm and the tree below 9 cm of the sapwood depth. The average sapwood depth, integrated flow, flow equivalent to TDP and the correction factor for the respective group is shown in Table 14.

Table 14 Factors for radial correction of sap flow in different categories of pine and natural trees

Fore stand	stand average Yx (cm)	average Yx (cm)			sap flow (cm <sup>3</sup> /hr)						Correction factor		
					considering the radial profile			TDP equivalent flow					
		I	II	III	I	II	III	I	II	III	I	II	III
PFS	10	7.63	10.57	12.8	300.9	460.5	545	407	781	1146	0.74	0.59	0.48
NFS	4.52	3.8	5.4		54.44	84.27		101	204		0.54	0.41	

Note: I, II, III represent group I, group II and group III of the respective stands

### 5.2.8. Temporal variability of transpiration at plot level

The stand level dry and wet season transpiration are presented in Table 15. The dry season transpiration is high in the pine forest compared to the wet season but the difference is not so big in natural forest compared to the pine forest. The annual transpiration in PFS (290 mm) is high as compared to the NFS (172 mm) which is attributable with the high water conducting area of sapwood. There is no big difference of dry and wet season daily transpiration in natural forest. Due to the high density of natural forest, the solar radiation penetration is very low throughout the year, thus moisture is retained in the soil. The rainy events in wet season reduce the transpiration due to reduced canopy conductance, thus giving lower value. The pine tree produces excessive resin during the wet season, continuously affecting the sensor, and thus the measurement. This was also continuously experienced during the field work. This might have underestimated transpiration in the pine during the wet season.

Table 15: Dry and wet season transpiration in PFS and NFS

Stand	Area (m <sup>2</sup> )	Species	No	ΣAx	Js (cm <sup>3</sup> hr <sup>-1</sup> cm <sup>-2</sup> )		Daily (mmd <sup>-1</sup> )		Total transpiration (mm)		Annual Transpiration (mm)
					dry	wet	dry	wet	dry	wet	
NFS	225	<i>Castanopsis tribuliodes</i>	13	1059.35	6.07	6.01	0.51	0.43	124	48	172
		<i>Schima wallachi</i>	4	333.72	2.93	3.22					
		<i>Quercus lamellosa</i>	3	175.26	3.98	6.28					
		<i>Rhododendron arboretum</i>	3	144.31	3.23	2.98					
		Kafal	3	243.34	2.10	2.10					
PFS	272	<i>Pinus roxburghii</i>	17	5535.98	3.21	1.35	1.00	0.42	243	47	290

Reminder: Dry-243 days from October-May, Wet-112 days from Jun-September

### 5.2.9. Spatial variability of transpiration

The BUF for the four locations in the pine forest in the study area and the correlation coefficient is shown in Fig 23. The spatial variability of transpiration in the pine forest was seen in the four different locations in the pine forest. The result shows that there is significant variation of the transpiration in the forest. The spatial variation is mostly attributed by size and density of trees. Though, a clear sky day was selected for the estimation of the transpiration, significant difference in the Humidity was found. Therefore, the environmental forcing has also shown the difference in the stand transpiration.

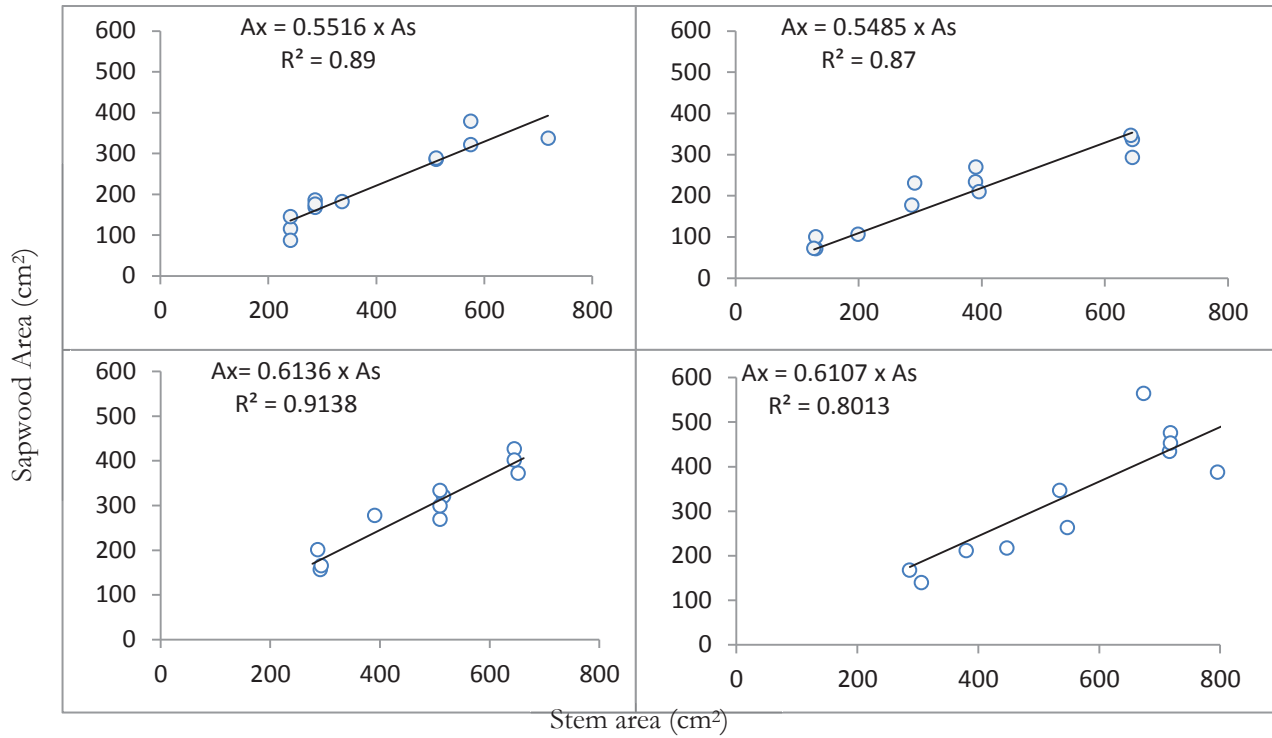


Figure 23: Derived BUF in four stands of pine

Table 16: Spatial variability of sap flow in the study area

	Stand 1	Stand 2	Stand 3	Stand 4
Study Period	14-March to 19-March	23-March to 29-March	4-April to 9-April	19-April to 24-April
Day selected	19-March	26-March	7-April	22-April
Duration of study [days]	6	7	6	6
Number of trees monitored	12	12	12	12
Plot size (m <sup>2</sup> )	15*16	15*15	20*20	18*15
Stem Density [per ha]	833	933	600	741
Average DBH(cm)	21.23	20.73	25.29	26.82
BUF (As vs Ax)	$A_x=0.55 \times A_s$	$A_x=0.55 \times A_s$	$A_x=0.61 \times A_s$	$A_x=0.61 \times A_s$
$R^2$ (As vs Ax)	0.89	0.87	0.91	0.8
Average Js (cm <sup>3</sup> hr <sup>-1</sup> cm <sup>-2</sup> )	4.78	5.77	4.19	3.35
$\sum A_x$ (cm <sup>2</sup> )	4062	4237	7185	7023
Average Rs(Wm <sup>-2</sup> )	242	232	222	264
RH	74	43	34	27
Average Tree transpiration [mmday <sup>-1</sup> ]	1.26	1.76	1.07	1.19

### 5.3. Evaporation from degraded soil

The HYDRUS is integrated with Rosetta Model which predicts the soil hydraulic properties based on the textural class and the bulk density by solving the van Genuchten-Maulem model. Thus, the textural class and the bulk density in the Table 17 were used to predict the initial guess of the parameters for calibration which are shown in Table 18.

Table 17: Textural properties and bulk density of soil in the degraded pasture land

Sand (%)	Silt (%)	Clay (%)	bulk density (gm/cm <sup>3</sup> )
15	65	20	1.21

The measured and modelled soil moisture in the soil profile is shown in Fig 24 and produce a very good result ( $R^2=0.96$ ) during calibration. The calibrated values are presented in Table 18. The model was validated from the moisture measurement in January and February, 2011 and gave a good validation result ( $R^2=0.66$ ).

Table 18: Initial parameters for Hydrus model simulation and associated objective function

Parameter	$\Theta_r$	$\Theta_s$	alpha	Ks (cm/day)	n	l
Initial guess	0.076	0.4683	0.005	43.29	1.6832	0.5
Calibration range	0.001-0.2	0.1-0.8	0.1-1	10-200	0-5	
Calibrated value	0.01	0.5	0.005623	11.985	1.6564	0.5

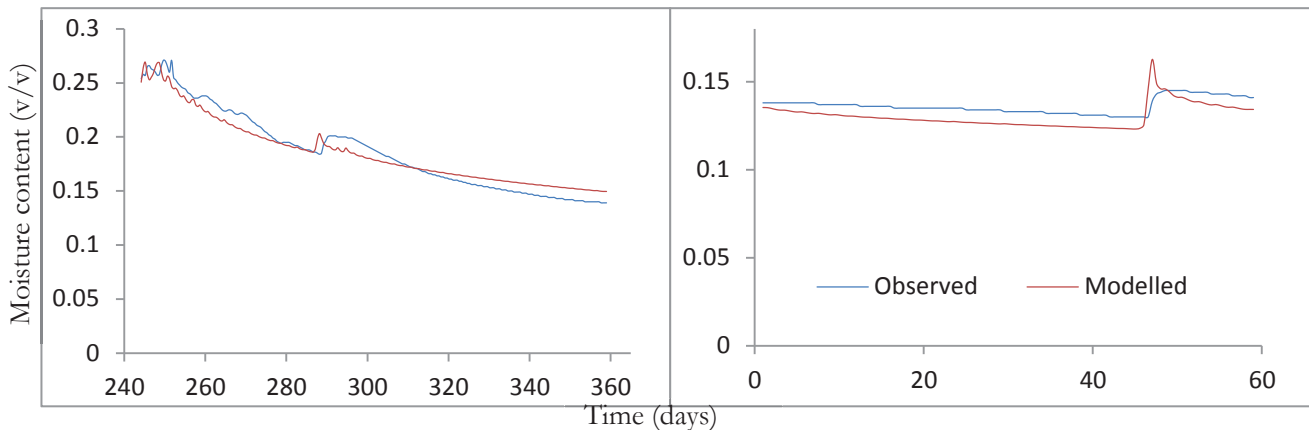


Figure 24: Observed and modelled soil moisture content during calibration (left) and validation (right) in Hydrus

The total dry and wet season top flux and bottom flux in the degraded soil is shown in Table 19. The result shows that the daily wet season flux is much higher than the dry season contributing more than half of the annual flux. During the dry season, there is less rainfall so the moisture continuously gets depleted and less and less water is available for evaporation. Thus, the dry season contribution to the annual evaporation is less. At the same time, after every rain events, most of the water is consumed by the unsaturated zone as more space is available for water. Thus the most of the bottom flux are evaporated back, thus contributing very less to the ground water recharge or interflow. However, the soil profile gets saturated faster as the moisture content in the profile will be high during the wet season. Thus, the most of the bottom flux contributes to restoring the soil moisture. This can also be seen from the Fig 25, the upper one represent the wet month June with 272 mm of rainfall in which there is continuous addition of

moisture to the soil profile while during January, the dry month with 5.52 mm of rainfall, there is continuous depletion of moisture. However, due to the increasing resistance of the soil at lower moisture content, the rate of evaporation continuously decreases.

Table 19: Total dry and wet season top and bottom flux in the degraded soil

	Top flux		Bottom Flux	
	Dry	Wet	Dry	Wet
Daily ( $\text{mmd}^{-1}$ )	0.38	0.93	0.28	1.57
Total (mm)	92.01	113.81	68.85	190.94
Grand total (mm)	205.82		259.79	

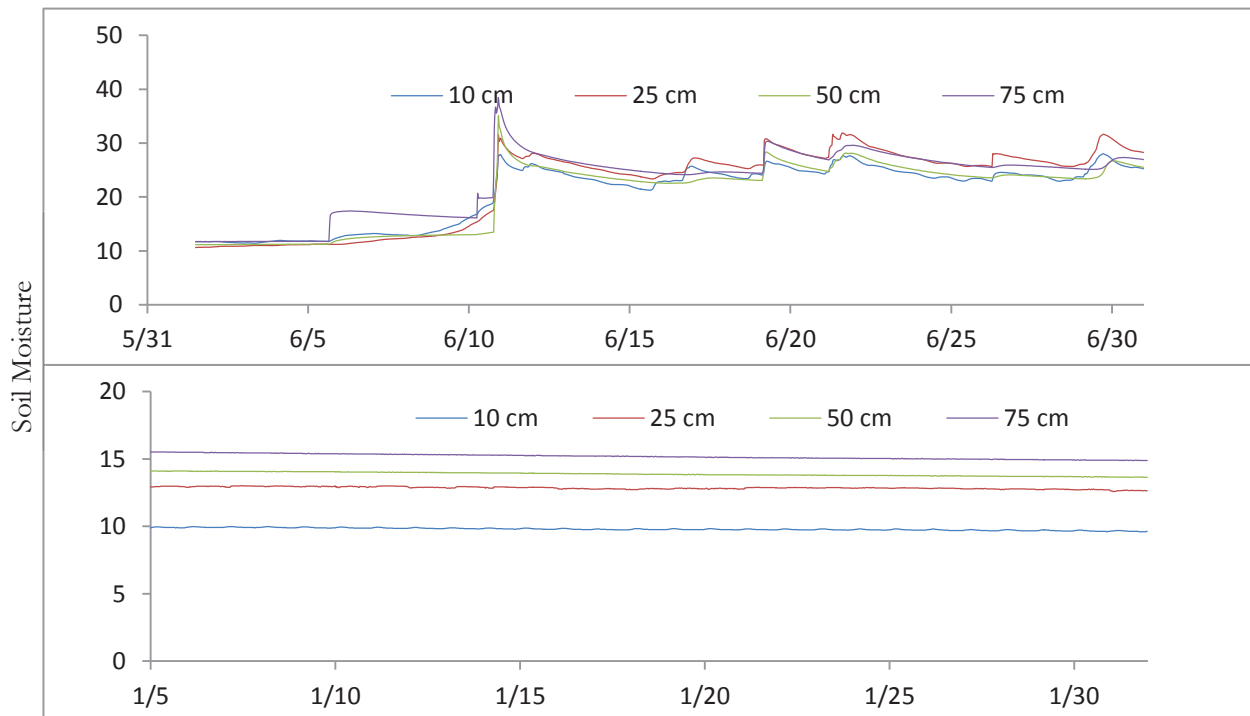


Figure 25: Soil moisture profile at 10 cm, 25 cm, 50 cm and 75 cm in June, 2011 (upper graph) and January, 2011 (lower graph)

#### 5.4. Annual evapotranspiration from natural forest, pine forest and degraded pasture

The overall ET contributed by the reforested pine stand, the original natural stands and the degraded stand representing the land cover before reforestation is shown in Table 20. This shows that the total ET in the planted pine forest is larger than the natural forest. The evaporation from the degraded soil is much lower than the pine and natural forest.

Table 20: Annual ET in PFS and NFS

	Transpiration (mm)		Evaporation (mm)		ET(mm)
	Dry	Wet	Dry	Wet	
PFS	243	47	68.89	207.19	566
NFS	124	48	84.59	238.39	495
DPL			92.01	113.81	206

### 5.5. Evapotranspiration from SEBS

The SEBS was run for the whole Jhikukhola catchment for two days. As the tree stands used for the transpiration and interception loss measurements were small and defining the boundary of the stands was difficult, therefore, a pixel representing the stands was selected based on the co-ordinate of Goggle earth. Mean evapotranspiration of nine pixels was taken with the values from centre pixel and the surrounding eight pixels. The comparison of SEBS ET of the two days of Landsat overpasses of 2 November 2010 and 22 February 2011 with corresponding ET estimated in stands are shown in Table 21. The result shows that in forested areas, the SEBS ET is significantly larger than the ET obtained from ground based transpiration and interception modelling. However, in degraded lands, the SEBS results are comparable with the output of HYDRUS.

In this study the forest ET was obtained as sum of tree transpiration obtained by upscaling of sap flow measurements and interception obtained by Gash Modelling. In that approach, the contribution of understory and the soil outside the access of the tree roots are neglected. This might have underestimated the total evaporation. In contrast, SEBS is highly sensitive to the gradient between land surface temperature and air temperature (Gibson *et al.*, 2011), so demands temperature measurements taken above canopy. However, it applies for other meteorological measurements also. The meteorological measurement at the degraded land at 3 m heights might not have been representative for the above canopy temperature, producing high difference in ET.

Table 21: Total ET (in  $\text{mmday}^{-1}$ ) obtained from SEBS and combined evaporation and interception modelling

Date	SEBS			Ground based modeling		
	Degraded soil	PFS	NFS	Degraded soil	PFS	NFS
2-Nov	1.04	2.76	3	0.74	1.00	0.53
22-Feb	2.55	3.69	2.81	1.93	1.09	0.56

## 6. DISCUSSIONS AND CONCLUSIONS

This study was carried out to understand the hydrological impact of reforestation through the measurement of evapotranspiration (ET). When analysed in combination with other components of water balance (WB), mainly rainfall, the ET gives ideas about how reforestation is influencing water balance. Therefore, three plots representing the original natural condition, degraded soil and the reforested area were selected. The contribution of the evaporation from the soil and the plants beneath the tree canopy in the forest to the overall ET is negligible and hence was neglected. The total forest ET was estimated as a sum of the evaporation of the intercepted rain and the transpiration from plants. The evaporation of the intercepted rain was estimated by using analytical Gash model and the transpiration from plants by sap flow measurements. These estimations were carried out in the two forest stands. The selection of these stands was a challenging issue because of large spatial variability of tree sizes and their densities. Therefore, the selection of the stands was primarily based on the average size and density of trees, and secondarily also on the area accessibility and local security. The two stands were selected close to each other so that the differences between the climatological and meteorological forcing becomes less significant so that the eventual difference in ET could then be attributed to different canopy characteristics and tree physiological properties. The ET results of the two forest stands were also compared with ET of degraded pasture land.

The Gash model of interception loss was applied in the pine and natural forest using the parameters derived by Ghimire *et al.* (2012) for the two stands. During the study period from October, 2010 to September, 2011, a total of 1482 mm of rainfall was recorded in the pine forest distributed over 169 events at an average of 8.77 mm per events. Similarly, a total of 1401 mm of rainfall distributed over 146 events at an average of 9.6 mm was recorded in the natural forest. The two stands are within distance of 3 kilometres, but receive a rainfall difference of almost 100 mm. This also shows the spatial variability of rainfall in the tropical forests. The total interception loss from the pine and natural forest estimated were 276 mm and 323 mm respectively representing 19 % and 23% respectively. High interception loss is as expected in the natural forest due to its high density.

The effect of the forest parameters on the interception model due to fixing the model parameters for the entire year is assumed to be minimal. The model was calibrated and validated during the wet season. The parameters developed during this period holds fairly true for the rest of the year. Slight changes in LAI occur when both forests sheds small proportion of their leaves. However, the effects of this changes on the annual interception loss is negligible because of the very low rainfall and hence the interception loss during that period. The wet canopy evaporation increased in the dry season due to higher wind speed and aerodynamic properties of the trees and reduced rainfall rate counterbalance the reduced storage capacity during the dry season thus maintaining small change in the net throughfall during wet and dry season (Herbst *et al.*, 2008).

The sensitivity analysis of the Gash model parameters shows that the most sensitive is the ratio  $\bar{E}/\bar{R}$ . This can be seen in the contribution of interception loss from saturated canopy; which represent more than 50% of the total interception loss. The wet canopy evaporation can be estimated using (Gash., 1979) or Penman-Montheith equation applying zero surface resistance. However, the first method gives comparably higher value than the later (Schellekens, 2000). Therefore, optimization of the wet canopy evaporation between the values from these two methods can produce better result.

The transpiration was estimated from the measurement of the sap flow. The presence of natural thermal gradient as well as radial, axial and circumferential variability of sap flux density was assessed. The effect of NTG was found minimal in the study area. This is due to the high density of trees and well shading canopy coverage of the both forest types. The circumferential and axial variability was also not found in the study area. The main causes of circumferential variability is the presence of isolated trees (Lu *et al.*, 2004) and water stress or water supply condition (Lu. *et al.*, 2000). Both of these conditions were not found in the sub-tropical humid climate prevailing in the Middle Mountains of Nepal. Similarly, the axial variability was limited by applying the sensors at the breast level.

The radial variability of sap flux density (Js) was found highly relevant in the study area. The Js varied significantly along the sapwood depth decreasing linearly towards the centre of xylem in *Pinus roxburghii* and exponentially in *Castanopsis tribuloides*. Assumption of uniform sap flow throughout the sapwood depth can introduce large error in the transpiration estimation. Several studies have reported the radial variation in sap flow some of them can be found in James *et al.* (2002), Fiora and Cescatti (2006), Ford *et al.* (2007), Poyatos *et al.* (2007) and Gebauer *et al.* (2008). The radial profile patterns are different in different literatures. The radial variability of Js seems to be a function of both species type, space (along the radial depth of sapwood) and time. The widely used and cost effective TDP method measures the sap flow at first 2 cm of the sapwood depth. If the sapwood depth is larger than 2 cm, the mean associated error was found to be 103 % for the investigated *Pinus roxburghii* and 139% for the investigated *Castanopsis tribuloides* respectively. The correction factor considering the ratio of radially integrated sap flow to TDP-based sap flow equivalent was estimated to be at 0.5 and 0.42 in *Pinus roxburghii* and *Castanopsis tribuloides* respectively. In order to make the correction factor more representative, the radial function was integrated to different sapwood depth to obtain correction factor for different categories of trees based on sapwood depth. Seasonal variability in the radial profile of the sap flux density was found by Fiora and Cescatti (2006) which is not accounted in the present study. Similarly, the correction factor developed in the dominant tree was applied for the other species, which may not be represented but the error associated with this can be considered minimum.

The measurement of sap flow in all the trees in the stand is not possible in the field and thus upscaling techniques was applied. For the annual transpiration, the upscaling needs to be done in spatial scale to upscale individual tree measurement to stand or catchment scale and temporal scale to model the temporal gaps from seasonal measurements. The study was carried out in a stand scale and measurement of the biometric properties of the trees was possible, so biometric upscaling function (BUF) from stem area to sapwood area were developed (Lubczynski, 2009). Some literatures are based on estimating sap flow using regression analysis between DBH and sap flow (García Santos, 2011; McJannet *et al.*, 2007). Second method is based on estimating sapwood area using the regression analysis between canopy area and stem area and separately calculating sap flow as a product of sapwood area and average sap flux density or sap flux density developed as a function with DBH (Ontiveros Enríquez, 2009). The second method was used in this study sap flux density in pine trees showed a very strong linear correlation with sap wood area ( $R^2=0.9$ ). However, the natural trees have a very poor trend so average sap flux density was applied. Similarly, the correlation coefficient ( $R^2$ ) between stem area and sapwood area in the pine and natural forest were respectively 0.89 and 0.96. The total sapwood area in the pine forest stand was estimated to be 5536 m<sup>2</sup>. Similarly, in the natural forest stand it was only 1956 m<sup>2</sup>.

The temporal extrapolation of the sap flux density is needed to fill the gaps for the periods when the measurements are not taken. Modelling the sap flux density applying environmental factors as an input can be a good approach (Ma *et al.*, 2008). Therefore the model developed by Cienciala *et al.* (2000) was applied as it is a simple model and consider the linear response of sap flux density with humidity and non-linear response with incoming solar radiation. The sap flux density showed a good correlation with solar radiation (Pearson coefficient: pine 0.71 and natural 0.89) and relative humidity (Pearson coefficient: pine

0.83 and natural 0.67), therefore application of the Cienfuegos model is applicable in the present study area. The model produced a good result but showed a poor correlation with the peaks. It could be due to the model deficiency for not accounting the important climatic factors such as wind speed.

The total transpiration from natural and pine forest stands are respectively 172 mm and 290 mm. High transpiration rate is expected in the pine forest as the sapwood area in the pine forest (5536 cm<sup>2</sup>) is much higher than the natural forest (1955.98 cm<sup>2</sup>).

One dimensional HYDRUS model was selected to estimate the degraded soil evaporation as it is simple and freely available software, also calibration of the model parameters can be done within its interface. The calibration of the model was done with the soil moisture data from September to December, 2010. The soil moisture measured at 10 cm, 25 cm, 50 cm and 100 cm soil depth was used. The initial guess predicted from the Rosetta Model integrated in the Hydrus for calibration. The calibration produced good correlation ( $R^2$ , 0.96). The model was validated with the soil moisture data from January 2011 to February 2011 and this validation produced a satisfactory result ( $R^2$ , 0.67). The model showed a quick response to the rainfall events.

The model was run on daily basis. The wet season top flux in the degraded soil was higher than the dry season evaporation due to the high moisture availability in the soil profile due to continuous rain events. However, the total evaporation was lower than the bottom flux thus the moisture was continuously added in the soil profile. But during the dry season, the top flux was more than the bottom flux, thus the moisture was continuously depleted. This was also seen from the observed moisture profile of a dry month and a wet month. During the dry month January, 2011, rainfall was very low (5.52 mm) and the moisture level in the soil profile was continuously depleting but in the wet month of June with rainfall of 272 mm, the continuous increase in the soil moisture content was observed. A total of 206 mm of top flux was obtained from the HYDRUS. Next to the combined ground based transpiration and interception modelling of ET, also remote sensing based ET applying SEBS algorithm was carried out in the study area. In the forests, pine and natural, the SEBS results show significantly larger ET than with ground based modelling where as in degraded it was comparable with the ET obtained from HYDRUS. This large differences over the forests are likely due to (i) possible underestimation of ground based ET because of neglecting transpiration of understory and evaporation of the soil outside the access of the tree roots, (ii) SEBS overestimation because of using meteorological measurements at 3 m height over the open space degraded land instead of using meteorological measurements above the forest canopy.

Comparison of ET in original natural forest, degraded pasture land and the reforested pine forest stand was done. The result of the study shows that the pine forest ET (566mm $yr^{-1}$ ) was the largest of the three types of land covers showing that the reforestation using pine trees has a significant effect on the total water balance. However, for the assessment of the overall hydrological impact of pine plantation, the other components of the water balance such as soil infiltration, runoff and ground water level need to be assessed. The degraded soil has evaporation of 206mm $yr^{-1}$  and is only 14% of the total rainfall. This means that most of the rainfall in the degraded soil contributes to the surface runoff or sub-surface flow. The ET from the natural forest is 495 mm. This shows that the reforesting the degraded land, increased water uptake by more than two times. The dry season transpiration (1mm $day^{-1}$ ) in the pine forest is much larger than the dry season transpiration (0.51mm $day^{-1}$ ) in the natural forest. The higher annual ET from the planted forest could be a contributory factor towards the drying water resources in the Middle Mountains of Nepal.

## 7. RECOMMENDATIONS

- The study was carried out to understand the hydrological impact of reforestation through the estimation of evapotranspiration. Selection of representative forest stand is a challenging and difficult task, particularly in complex and rugged topography (i.e. present study area). Therefore, use of remote sensing for the upscaling of plot measurement into the catchment can be a better option.
- The radial correction factor used for the TDP measurement is based on the measurement for few days. Temporal variation of radial profile is mentioned in some literatures. Therefore, season based radial profile is recommended when transpiration estimation is needed for a complete hydrological year.
- Very limited work has been done for the extrapolation of sap flux densities. The Cienciala model used in the present study is based on solar radiation and relative humidity and the model doesn't take into account the effect of wind speed and plant physiological properties. Hence model that takes into account all the climatological factors and tree physiological property is recommended.

## LIST OF REFERENCES

- Adnan, N. A., & Atkinson, P. M. (2011). Exploring the impact of climate and land use changes on streamflow trends in a monsoon catchment. *International Journal of Climatology*, 31(6), 815-831.
- Allen, R. G., Pereira, L. S., Raes, D., & Smith, M. (1998). *Crop Evapotranspiration-Guidelines for computing crop water requirements* (Vol. 56): FAO.
- Baker, J. M., & Van Bavel, C. H. M. (1987). Measurement of mass flow of water in the stems of herbaceous plants. *Plant, Cell & Environment*, 10(9), 777-782.
- Bernier, P. Y., Bréda, N., Granier, A., Raulier, F., & Mathieu, F. (2002). Validation of a canopy gas exchange model and derivation of a soil water modifier for transpiration for sugar maple (*Acer saccharum* Marsh.) using sap flow density measurements. *Forest Ecology and Management*, 163(1-3), 185-196. doi: 10.1016/s0378-1127(01)00578-3
- Bieker, D., & Rust, S. (2010). Non-Destructive Estimation of Sapwood and Heartwood Width in Scots Pine (*Pinus sylvestris* L.). [Research article]. *Silva Fennica*, 44(2), 267-273.
- Bosch, J. M., & Hewlett, J. D. (1982). A review of catchment experiments to determine the effect of vegetation changes on water yield and evapotranspiration. *Journal of Hydrology*, 55(1-4), 3-23.
- Bruijnzeel, L. A. (2004). Hydrological functions of tropical forests: not seeing the soil for the trees? *Agriculture, Ecosystems & Environment*, 104(1), 185-228.
- Bruijnzeel, L. A., Sampurno, S. P., & Wiersum, K. F. (1987). Rainfall interception by a young *Acacia auriculiformis* (a. cunn) plantation forest in West Java, Indonesia: Application of Gash's analytical model. *Hydrological Processes*, 1(4), 309-319. doi: 10.1002/hyp.3360010402
- Burrough, P. A. (1989). Matching spatial databases and quantitative models in land resource assessment. *Soil Use and Management*, 5(1), 3-8.
- Calder, I. R., & Rosier, P. T. W. (1976). Design of large plastic-sheet net-rainfall gauges *Journal of Hydrology*, 30(4), 403-405.
- Cammalleri, C., Agnese, C., Ciraolo, G., Minacapilli, M., Provenzano, G., & Rallo, G. (2010). Actual evapotranspiration assessment by means of a coupled energy/hydrologic balance model: Validation over an olive grove by means of scintillometry and measurements of soil water contents. *Journal of Hydrology*, 392(1-2), 70.
- Čermák, J., & Kučera, J. (1981). The compensation of natural temperature gradient at the measuring point during the sap flow rate determination in trees. *Biologia Plantarum*, 23(6), 469-471.
- Čermák, J., Kučera, J., & Nadezhdina, N. (2004). Sap flow measurements with some thermodynamic methods, flow integration within trees and scaling up from sample trees to entire forest stands. *Trees - Structure and Function*, 18(5), 529-546.
- Chanzy, A., & Bruckler, L. (1993). Significance of soil surface moisture with respect to daily bare soil evaporation. *Water Resour. Res.*, 29(4), 1113-1125.
- Cienciala, E., Kucera, J., & Malmer, A. (2000). Tree sap flow and stand transpiration of two *Acacia mangium* plantations in Sabah, Borneo. *Journal of Hydrology*, 236(1-2), 109-120.
- Clarke, R. T. (1986/87). The Interception Process in Tropical Rain Forest: A literature review and critique. [Review]. *Acta Amazonica*, 16/17, 225-237.
- Courault, D., Seguin, B., & Olioso, A. (2005). Review on estimation of evapotranspiration from remote sensing data: From empirical to numerical modeling approaches. *Irrigation and Drainage Systems*, 19(3), 223-249.
- Crockford, R. H., & Richardson, D. P. (2000). Partitioning of rainfall into throughfall, stemflow and interception: effect of forest type, ground cover and climate. *Hydrological Processes*, 14(16-17), 2903-2920.
- Deme, G. (2011). *Partitioning subsurface water fluxes using coupled hydrus - modflow model : case study of La Mata catchment, Spain*. University of Twente Faculty of Geo-Information and Earth Observation ITC, Enschede (Msc Thesis). Retrieved from [http://www.itc.nl/library/papers\\_2011/msc/wrem/deme.pdf](http://www.itc.nl/library/papers_2011/msc/wrem/deme.pdf)
- Do, F., & Rocheteau, A. (2002a). Influence of natural temperature gradients on measurements of xylem sap flow with thermal dissipation probes 2 : advantages and calibration of noncontinuous heating system. In: *Tree Physiology*, 22(2002), pp. 649-654.

- Do, F., & Rocheteau, A. (2002b). Influence of natural temperature gradients on measurements of xylem sap flow with thermal dissipation probes 1: field observations and possible remedies. *In: Tree Physiology*, 22(2002), pp. 641-648.
- Dolman, A. J. (1987). Summer and winter rainfall interception in an oak forest. Predictions with an analytical and a numerical simulation model. *Journal of Hydrology*, 90(1-2), 1-9.
- Dugas, W. A., Fritschen, L. J., Gay, L. W., Held, A. A., Matthias, A. D., Reicosky, D. C., . . . Steiner, J. L. (1991). Bowen-ratio, eddy-correlation and portable chamber measurements of sensible and latent heat flux over irrigated spring wheat *Agricultural and Forest Meteorology*, 56(1-2), 1-20.
- Dynamax Inc. (1997). A thermal dissipation sap velocity probe for measurement of sap flow in plants. In I. Dynamax (Ed.), *Manual*. Houston: Dynamax, Inc.
- Fernandez, E. (2011). Method to Estimate Sap Flow. *ISHS Working Group on Sap flow*. Retrieved 15/08/2011, from <http://www.wgsapflow.com/methods.pdf>
- Fiora, A., & Cescatti, A. (2006). Diurnal and seasonal variability in radial distribution of sap flux density: implications for estimating stand transpiration. *Tree Physiology*, 26(9), 1217-1225.
- Ford, C. R., Hubbard, R. M., Kloeppel, B. D., & Vose, J. M. (2007). A comparison of sap flux-based evapotranspiration estimates with catchment-scale water balance. *Agricultural and Forest Meteorology*, 145(3-4), 176-185.
- Ford, C. R., McGuire, M. A., Mitchell, R. J., & Teskey, R. O. (2004). Assessing variation in the radial profile of sap flux density in Pinus species and its effect on daily water use. *Tree Physiology*, 24(3), 241-249.
- Fregoso, A. (2002). *Dry - season transpiration of Savannah vegetation : assessment of tree transpiration and its spatial distribution in Serowe, Botswana*. Msc Thesis, ITC, Enschede. Retrieved from [http://www.itc.nl/library/papers/msc\\_2002/nrm/fregoso.pdf](http://www.itc.nl/library/papers/msc_2002/nrm/fregoso.pdf)
- García Santos, G. (2011). Transpiration in a sub-tropical ridge-top cloud forest. *Journal of Hydrology*(0).
- Gash, J. H. C., & Morton, A. J. (1978). Application of Rutter model to estimation of interception loss from theford forest. *Journal of Hydrology*, 38(1-2), 49-58.
- Gash, J. H. C., Wright, I. R., & Lloyd, C. R. (1980). Comparative estimates of interception loss from three coniferous forests in Great Britain. *Journal of Hydrology*, 48(1-2), 89-105.
- Gash, J. (1979). analytical model of rainfall interception by forests. *In: Quarterly journal of the royal meteorological society*, 105(1979)443, pp. 43-55.
- Gash, J., Lloyd, C. R., & Lachaud, G. (1995). Estimating sparse forest rainfall interception with an analytical model. *Journal of Hydrology*, 170(1-4), 79-86.
- Gebauer, T., Horna, V., & Leuschner, C. (2008). Variability in spatial sap flux density patterns and sapwood area among seven co-occurring temperate broad-leaved tree species. *Tree Physiology*, 28, 1821-1830.
- Ghimire, C. P., Bruijnzeel, L. A., Lubczynski, M., & Bonel, M. (2012). in preparation: Rainfall interception by natural and planted forest in the Middle Mountains of central Nepal. *Hydrological Sciences*
- Gibson, L. A., Munch, Z., & Engelbrecht, J. (2011). Particulate uncertainties encountered in using a pre-packed SEBS model to derive evapotranspiration in a heterogeneous study area in South Africa. *Hydrol. Earth System. Sci*, 15(1), 295-310.
- Goulden, M. L., & Field, C. B. (1994). Three methods for monitoring gas exchange of individual tree canopies: ventilated-chamber, sap-flow and Penman-Montheith measurements on evergreen oaks. [Technical Report]. *Functional ecology*, 8(125-135).
- Granier, A. (1987). Evaluation of Transpiration in a Douglas-fir stand by means of sap flow measurements. *Tree Physiology*, 3, 309-320.
- Granier, A., Biron, P., Breda, N., Pontailler, J. Y., & Saugier, B. (1996). Transpiration of trees and forest stands: Short and longterm monitoring using sapflow methods. [Article]. *Global Change Biology*, 2(3), 265-274.
- Grebet, P., & Cuenca, R. H. (1991). *History of lysimeter design and effects of environmental disturbances*.
- Hatton, T. J., Catchpole, E. A., & Vertessy, R. A. (1990). Integration of sapflow velocity to estimate plant water use. *In: Tree Physiology*, 6(1990), pp. 201-209.
- Helvey, J., & Patric, J. (1965). Canopy and Litter Interception of Rainfall by Hardwoods of Eastern United States. *Water Resour. Res.*, 1(2), 193-206.
- Herbst, M., Rosier, P. T. W., McNeil, D. D., Harding, R. J., & Gowing, D. J. (2008). Seasonal variability of interception evaporation from the canopy of a mixed deciduous forest. *Agricultural and Forest Meteorology*, 148(11), 1655-1667.

- Herron, N., Davis, R., & Jones, R. (2002). The effects of large-scale afforestation and climate change on water allocation in the Macquarie River catchment, NSW, Australia. *Journal of Environmental Management*, 65(4), 369-381.
- Hutjes, R. W. A., Wierda, A., & Veen, A. W. L. (1990). Rainfall interception in the Tai Forest, Ivory Coast: Application of two simulation models to a humid tropical system. *Journal of Hydrology*, 114(3-4), 259-275.
- ICT International. (2011a). Heat Field Deformation Sap Flow, from <http://www.ictinternational.com.au/brochures/hfd.pdf>
- ICT International. (2011b). Sap Flow Tool: analysis and visualization of sap flow data Retrieved 2011-11-15, 2011
- Isarangkool, S., Ayuthaya, N. A., Do, F. C., Pannegetch, K., Jundittakarn, J., Maeght, J. L., . . . Cochard, H. (2009). Transient thermal dissipation method of xylem sap flow measurement: multi-species calibration and field evaluation. *Tree Physiology*, 30, 139-148.
- Jackson, I. J. (1975). Relationships between rainfall parameters and interception by tropical forest. *Journal of Hydrology*, 24(3-4), 215-238.
- James, S. A., Clearwater, M. J., Meinzer, F. C., Goldstein, G., , & (2002). Heat dissipation sensors of variable length for the measurement of sap flow in trees with deep sapwood. *Tree Physiology*, 22, 277-283.
- Jones, H. G., Hamer, P. J. C., & Higgs, K. H. (1988). Evaluation of various heat-pulse methods for estimation of sap flow in orchard trees: comparison with micrometeorological estimates of evaporation. *Trees - Structure and Function*, 2(4), 250-260.
- Karkee, K. (2004). *Land Degradation in Nepal: A Menace to Economy and Ecosystems*. . International Master's Programme in Environmental Science (LUMES), Lund University, Lund, Sweden.
- Klocke, N. L., Heermann, D. F., & Duke, H. R. (1985). Measurement of evaporation and transpiration with lysimeters *Transactions of the Asae*, 28(1), 183-&.
- Komatsu, H., Kume, T., & Otsuki, K. (2011). Increasing annual runoff—broadleaf or coniferous forests? *Hydrological Processes*, 25(2), 302-318.
- Komatsu, H., Kume, T., & Otsuki, K. (2009). Changes in low flow with the conversion of a coniferous plantation to a broad-leaved forest in a summer precipitation region, Japan. *Ecobydrology*, 2(2), 164-172.
- Köstner, B., Granier, A., & Cermák, J. (1998). Sapflow measurements in forest stands: methods and uncertainties. *Ann. For. Sci.*, 55(1-2), 13-27.
- Kumagai, T. o., Aoki, S., Nagasawa, H., Mabuchi, T., Kubota, K., Inoue, S., . . . Otsuki, K. (2005). Effects of tree-to-tree and radial variations on sap flow estimates of transpiration in Japanese cedar. *Agricultural and Forest Meteorology*, 135(1-4), 110-116.
- Kustas, W. P., & Daughtry, C. S. T. (1990). Estimation of the soil heat flux/net radiation ratio from spectral data. *Agricultural and Forest Meteorology*, 49(3), 205-223.
- Liu, G. S., & Liu, Y. (2007). *Validation of the Penman-Monteith model with estimated radiation*.
- Lloyd, C. R., Gash, J. H. C., Shuttleworth, W. J., & de O. Marques F, A. (1988). The measurement and modelling of rainfall interception by Amazonian rain forest. *Agricultural and Forest Meteorology*, 43(3-4), 277-294.
- Lu, P., Urban, L., & Ping, Z. (2004). Granier's Thermal Dissipation Probe (TDP) Method for Measuring Sap Flow in Trees: Theory and Practice. [Review]. *Science China Press*, 46(6), 631-646.
- Lu, P., Muller, W. J., & Chacko, E. K. (2000). Spatial variations in xylem sap flux density in the trunk of orchard-grown, mature mango trees under changing soil water conditions. *Tree Physiology*, 20(10), 683-692.
- Lubczynski. (2000). Groundwater evapotranspiration, underestimated component of the groundwater balance in a semi - arid environment, Serowe case, Botswana. *In: Groundwater : past achievements and future challenges / ed. by O. Sililo...[et al.]. Balkema Rotterdam, 2000. ISBN 9058091597 pp. 199-204.*
- Lubczynski. (2009). The hydrogeological role of trees in water-limited environments. *Hydrogeology Journal*, 17(1), 247-259.
- Lui, H., & Foken, T. (2001). A modified Bowen ratio method to determine sensible and latent heat fluxes. *Meteorologische Zeitschrift*, 10(1), 71-80.
- Ma, L., Lu, P., Zhao, P., Rao, X.-q., Cai, X.-a., & Zeng, X.-p. (2008). Diurnal, daily, seasonal and annual patterns of sap-flux-scaled transpiration from an *Acacia mangium* plantation in South China. *Ann. For. Sci.*, 65(4), 402.

- Marshall, D. C. (1958). Measurement of sap flow in conifers by heat transport. *Plant Physiology*, 33(6), 385-396.
- McJannet, D., Fitch, P., Disher, M., & Wallace, J. (2007). Measurements of transpiration in four tropical rainforest types of north Queensland, Australia. [Article]. *Hydrological Processes*, 21(26), 3549-3564.
- Merz, J. (2004). *Water Balances, Floods and Sediment Transport in the Hindu Kush-Himalayas: Data analysis, modelling and comparison of selected meso-scale catchments*. PhD dissertation, University of Bern, Switzerland. (PhD dissertation)
- Monteith. (1965). Evaporation and the environment. In: *Symposium of the society for experimental biology*, 19(2965), pp. 203-234.
- Monteith., & Unsworth, M. (2008). *Principles of environmental physics* (Third edition ed.). Amsterdam etc.: Elsevier.
- Nadezhdina, N., Cermak, J., & Ceulemans, R. (2002a). Radial patterns of sap flow in woody stems of dominant and understory species : scaling errors associated with positioning of sensors. In: *Tree physiology : an international journal*, 22(2002), pp. 907-918.
- Nadezhdina, N., Cermak, J., & Ceulemans, R. (2002b). Radial patterns of sap flow in woody stems of dominant and understory species: scaling errors associated with positioning of sensors. *Tree Physiology*, 22(13), 907-918.
- Ontiveros Enríquez, R. (2009). *Tree transportation : a spatio - temporal approach in water limited environments, Sardon study case*. Msc Thesis, ITC, Enschede. Retrieved from [http://www.itc.nl/library/papers\\_2009/msc/wrem/enriquez.pdf](http://www.itc.nl/library/papers_2009/msc/wrem/enriquez.pdf)
- Parrotta, J. A. (1992). The role of plantation forests in rehabilitating degraded tropical ecosystems. *Agriculture, Ecosystems & Environment*, 41(2), 115-133.
- Pearce, A. J., & Rowe, L. K. (1981). Rainfall Interception In A Multi-Storied, Evergreen Mixed Forest: Estimates Using Gash's Analytical Model. *Journal of Hydrology*, 49(3-4), 341-353.
- Pereira, F. L., Gash, J. H. C., David, J. S., David, T. S., Monteiro, P. R., & Valente, F. (2009). Modelling interception loss from evergreen oak Mediterranean savannas: Application of a tree-based modelling approach. *Agricultural and Forest Meteorology*, 149(3-4), 680-688.
- Poyatos, R., Čermák, J., & Llorens, P. (2007). Variation in the radial patterns of sap flux density in pubescent oak (*Quercus pubescens*) and its implications for tree and stand transpiration measurements. *Tree Physiology*, 27(4), 537-548.
- Qiu, G. Y., Yano, T., & Momii, K. (1998). An improved methodology to measure evaporation from bare soil based on comparison of surface temperature with a dry soil surface. *Journal of Hydrology*, 210(1-4), 93-105.
- Rana, G., & Katerji, N. (2000). Measurement and estimation of actual evapotranspiration in the field under Mediterranean climate: a review. *European Journal of Agronomy*, 13(2-3), 125-153.
- Reicosky, D. C., & Peters, D. B. (1977). A Portable Chamber for Rapid Evapotranspiration Measurements on Field Plots. *Agron. J.*, 69(4), 729-732.
- Reyes, J. L. R. A., Vandegehuchte, M., Steppe, K., & Lubczynski, M. W. (2011). Natural temperature gradients bias on Thermal Dissipation, TDP, probes and Heat Field Deformation sensors (HFD) : dynamics and correction by applying a cyclic thermal dissipation methodology : powerpoint. Presented at 8th international workshop on sap flow, Volterra, Italy, 8-12 May 2011.21 slides.
- Riekerk, H. (1989). Influence of silvicultural practices on the hydrology of pine flatwoods in Florida. *Water Resour. Res.*, 25(4), 713-719.
- Rincon, D. C., Su, Z., & Lubczynski, M. W. (2009). *Tree transpiration mapping from upscaled sap flow in the Botswana Kalahari*. 159, ITC University of Twente, Enschede. Retrieved from [http://www.itc.nl/library/papers\\_2009/phd/chavarro.pdf](http://www.itc.nl/library/papers_2009/phd/chavarro.pdf)
- Rust, S. (1999). Comparison of three methods for determining the conductive xylem area of Scots pine (*Pinus sylvestris*). *Forestry*, 72(2), 103-108.
- Rutter, A. J., Kershaw, K. A., Robins, P. C., & Morton, A. J. (1971). A predictive model of rainfall interception in forests, 1. Derivation of the model from observations in a plantation of Corsican pine. *Agricultural Meteorology*, 9(0), 367-384. doi: 10.1016/0002-1571(71)90034-3
- Rutter, A. J., Robins, P. C., Morton, A. J., & Kershaw, K. A. (1972). Predictive model of rainfall interception in forests. 1. Derivation of model from observations in a plantation of corsican pine. *Agricultural Meteorology*, 9(5-6), 367-&.
- Schellekens, J. (2000). *Hydrological processes in a humid tropical rain forest: a combined experimental and modelling approach*. Ph D Ph D thesis, Vrije Universiteit, Amsterdam.

- Schellekens, J., Scatena, F. N., Bruijnzeel, L. A., & Wickel, A. J. (1999). Modelling rainfall interception by a lowland tropical rain forest in northeastern Puerto Rico. *Journal of Hydrology*, 225(3-4), 168-184.
- Schurr, U. (1998). Xylem sap sampling - new approaches to an old topic. *Trends in Plant Science*, 3(8), 293-298.
- Shunlin, L. (2001). Narrowband to broadband conversions of land surface albedo I: Algorithms. *Remote Sensing of Environment*, 76(2), 213-238. doi: 10.1016/S0034-4257(00)00205-4
- Silva, I., & Okumura, T. (1996). Throughfall, stemflow and interception loss in a mixed white oak forest (<i>Quercus serrata</i> Thunb.). *Journal of Forest Research*, 1(3), 123-129.
- Simunek, J., Sejna, H., Saito, H., Sakai, M., & Genuchten, M. (2009). The HYDRUS-1D software package for simulating the One-dimensional movement of water, heat and multiple solute in variably saturated media. California: University of California.
- Šimůnek, J., & van Genuchten, M. T. (2008). Modeling Nonequilibrium Flow and Transport Processes Using HYDRUS. *Vadose Zone J.*, 7(2), 782-797.
- Simunek, J., van Genuchten, M. T., & Sejna, M. (2008). Development and applications of the HYDRUS and STANMOD software packages and related codes. In: *Vadose zone journal*, 7(2008)2, pp. 587-600.
- Smith, D. M., & Allen, S. J. (1996). Measurement of sap flow in plant stems. *Journal of Experimental Botany*, 47(305), 1833-1844.
- Steppe, K., De Pauw, D. J. W., Doody, T. M., & Teskey, R. O. (2010). A comparison of sap flux density using thermal dissipation, heat pulse velocity and heat field deformation methods. *Agricultural and Forest Meteorology*, 150(7-8), 1046-1056.
- Steward, J. B. (1989). *On the use of the Penman-Monteith equation for determining areal evapotranspiration*. Paper presented at the Estimation of Areal Evapotranspiration, Vancouver, B.C., Canada.
- Stormount, J., & Coonrod, J. (2004). *Water depletions from soil evaporation*. Identifying Technologies to Improve Regional Water Stewardship: North-Middle Rio Grande Corridor The University of New Mexico.
- Stroosnijder, L. (1987). Soil evaporation: test of a practical approach under semi-arid conditions. *Netherlands Journal of Agricultural Science*, 35, 417-426.
- Su, Z. (2002). The Surface Energy Balance System (SEBS) for estimation of turbulent heat fluxes. *Hydrology and Earth System Sciences*, 6(1), 16.
- Sun, G., McNulty, S. G., Lu, J., Amatya, D. M., Liang, Y., & Kolka, R. K. (2005). Regional annual water yield from forest lands and its response to potential deforestation across the southeastern United States. *Journal of Hydrology*, 308(1-4), 258-268.
- Trabucco, A., Zomer, R., Bossio, D., van Straaten, O., & Verchot, L. (2008). Climate change mitigation through afforestation/reforestation: A global analysis of hydrologic impacts with four case studies. *Agriculture, Ecosystems & Environment*, 126(1-2), 81-97.
- University of California. (2012). Vadose Zone Modeling Retrieved 2012-01-05, 2012, from <http://groundwater.ucdavis.edu/vadzonemodels.htm>
- Valente, F., David, J. S., & Gash, J. H. C. (1997). Modelling interception loss for two sparse eucalypt and pine forests in central Portugal using reformulated Rutter and Gash analytical models. *Journal of Hydrology*, 190(1-2), 141-162.
- Valor, E., & Caselles, V. (1996). Mapping land surface emissivity from NDVI: Application to European, African, and South American areas. *Remote Sensing of Environment*, 57(3), 167-184. doi: 10.1016/0034-4257(96)00039-9
- Wilson, K. B., Hanson, P. J., Mulholland, P. J., Baldocchi, D. D., & Wullschleger, S. D. (2001). A comparison of methods for determining forest evapotranspiration and its components: sap-flow, soil water budget, eddy covariance and catchment water balance. *Agricultural and Forest Meteorology*, 106(2), 153-168.
- Xiaohua, W., James, V., Zhiqiang, Z., Guoyi, Z., Steven, M., & Ge, S. (2007). Forest And Water Relations Hydrologic Implications Of Forestation Campaigns In China *Wetland and Water Resource Modeling and Assessment* (pp. 71-88): CRC Press.

ANNEX A: Biometric characteristics of natural and pine forest stands with Biometric upscaling function

PINE FOREST STAND (BUF: $A_x=0.5214 \cdot A_s+16.568$ ) $R^2=0.89$					
S.No.	Circumference	DBH	stem area	sapwood area	Species
1	100	31.8	794.23	593.96	<i>Pinus roxburghii</i>
2	83	26.4	547.39	330.06	<i>Pinus roxburghii</i>
3	85	27.1	576.80	363.05	<i>Pinus roxburghii</i>
4	70	22.3	390.57	226.98	<i>Pinus roxburghii</i>
5	91	29	660.52	363.05	<i>Pinus roxburghii</i>
6	95	30.2	716.31	380.13	<i>Pinus roxburghii</i>
7	98	31.2	764.54	383.60	<i>Pinus roxburghii</i>
8	75	23.9	448.63	201.06	<i>Pinus roxburghii</i>
9	56	17.8	248.85	113.10	<i>Pinus roxburghii</i>
10	80	25.5	510.71	298.65	<i>Pinus roxburghii</i>
11	62	19.7	304.81	201.06	<i>Pinus roxburghii</i>
12	106	33.7	891.97	481.64	<i>Pinus roxburghii</i>
13	81	25.8	522.79	289.15	<i>Pinus roxburghii</i>
14	65	20.7	336.54	192.04	<i>Pinus roxburghii</i>
15	94	29.9	702.15	382.67	<i>Pinus roxburghii</i>
16	77	24.5	471.44	262.37	<i>Pinus roxburghii</i>
17	105	33.4	876.16	473.40	<i>Pinus roxburghii</i>
NATURAL FOREST STAND (BUF: $A_x=0.3971 \cdot A_s+30.963$ ) $R^2=0.96$ (only for M.Katus)					
1	49.64	15.8	196.07	108.75	<i>Castanopsis tribuliodes</i>
2	38.96	12.4	120.76	76.98	<i>Castanopsis tribuliodes</i>
3	29.53	9.4	69.40	67.93	<i>Quercus lamellose</i>
4	39.90	12.7	126.68	84.38	<i>Castanopsis tribuliodes</i>
5	36.13	11.5	103.87	66.59	<i>Castanopsis tribuliodes</i>
6	34.24	10.9	93.31	72.38	<i>Castanopsis tribuliodes</i>
7	35.81	11.4	102.07	67.74	<i>Quercus lamellose</i>
8	48.69	15.5	188.69	105.68	<i>Schima wallachi</i>
9	49.95	15.9	198.56	109.96	<i>Castanopsis tribuliodes</i>
10	27.65	8.8	60.82	39.59	<i>Quercus lamellose</i>
11	48.38	15.4	186.27	41.85	<i>Castanopsis tribuliodes</i>
12	43.35	13.8	149.57	114.99	<i>Myrica esculenta</i>
13	32.67	10.4	84.95	54.11	<i>Schima wallachi</i>
14	29.53	9.4	69.40	50.27	<i>Rhododendron arborestum</i>
15	33.93	10.8	91.61	58.09	<i>Rhododendron arborestum</i>
16	131.95	42	1385.44	581.12	<i>Castanopsis tribuliodes</i>
17	157.08	50	1963.50	810.67	<i>Castanopsis tribuliodes</i>
18	94.25	30	706.86	311.66	<i>Castanopsis tribuliodes</i>
19	113.10	36	1017.88	517.86	<i>Schima wallachi</i>
20	84.82	27	572.56	440.18	<i>Myrica esculenta</i>
21	116.24	37	1075.21	826.62	<i>Myrica esculenta</i>

22	147.65	47	1734.94	719.91	<i>Castanopsis tribuloides</i>
23	157.08	50	1963.50	987.92	<i>Schima wallachi</i>
24	91.11	29	660.52	293.26	<i>Castanopsis tribuloides</i>
25	59.69	19	283.53	125.66	<i>Rhododendron arborestum</i>
26	128.81	41	1320.25	555.24	<i>Castanopsis tribuloides</i>

## ANNEX 2: Parameter estimation and corresponding errors in Cienicala Model

Forest stand	Season	Tree ID	Parameters			Objective Function			
			a	b	c	Calibration		Validation	
						RMSE (cmhr-1)	MAE (cmhr-1)	RMSE (cmhr-1)	MAE (cmhr-1)
PFS	Dry	Tree 1	0.274	0.959	0.228	1.338	0.698	4.130	1.141
		Tree 2	0.300	0.990	1.350	1.679	0.718	1.357	0.629
		Tree 4	0.360	0.980	1.450	0.851	0.445	1.065	0.583
		Tree 4b	0.450	0.980	1.469	1.525	0.817	2.103	1.447
		Tree 5	0.250	0.950	1.240	0.891	0.481	1.604	0.853
		Tree 6b	0.100	0.299	1.903	0.679	0.350	0.807	0.381
	Wet	Tree 1	0.300	0.180	3.220	1.467	0.780	1.188	0.638
		Tree 2	0.360	0.900	1.950	1.467	0.485	1.010	0.469
		Tree 3	0.290	0.900	2.220	0.560	0.296	0.891	0.379
		Tree 4	0.250	0.800	1.600	1.012	0.528	0.862	0.438
		Tree 5	0.150	0.980	1.580	0.338	0.177	1.576	0.680
		Tree 6	0.200	0.700	3.210	0.556	1.283	0.733	0.381
NFS	Dry	Tree 1	0.292	0.617	0.412	2.097	1.098	8.753	5.417
		Tree 2	0.701	0.938	1.037	1.225	0.589	3.296	1.744
		Tree 3	0.160	0.280	0.728	1.292	0.692	1.500	0.839
		Tree 4	0.690	0.920	1.250	1.156	0.573	3.100	1.705
		Tree 5	0.250	0.397	1.810	3.164	1.271	1.765	1.003
		Tree 6	0.325	0.231	2.379	1.043	0.530	0.911	0.480
		Tree 7	0.487	1.053	1.789	1.128	0.605	1.563	0.831
		Tree 8	0.437	0.873	2.259	1.914	0.940	1.887	1.073
		Tree 9	0.100	0.299	1.903	6.567	3.224	4.818	1.837
		Tree 9c	0.207	0.980	1.181	1.204	0.688	0.954	0.570
		Tree 7b	0.341	0.832	1.173	1.485	0.792	1.252	0.720
		Tree 4b	0.340	0.991	0.858	1.468	0.746	1.116	0.633
	Wet	Tree 1	0.841	0.688	2.481	1.492	0.780	2.317	1.242
		Tree 2	0.562	0.880	0.266	1.671	0.895	1.827	0.966
		Tree 3	0.751	0.852	0.867	1.744	0.920	1.771	0.934
		Tree 4	0.458	0.812	0.380	1.480	0.820	1.394	0.753
		Tree 5	0.999	0.983	0.996	1.580	0.767	1.680	0.771
		Tree 6	0.594	0.912	1.450	1.118	0.535	1.409	0.725
		Tree 8	0.646	0.993	1.002	1.008	0.494	1.485	0.751
		Tree 9	0.565	0.961	0.773	0.918	0.443	1.178	0.609

